

Supporting Information for

2D Assignment and Quantitative Analysis of Nanocellulose and Oxidized Nanocelluloses using Solution-State NMR Spectroscopy

T. Koso*, D. Rico del Cerro, S. Heikkinen, T. Nypelö, J. Buffiere, J. E. Perea-Buceta, A. Potthast, T. Rosenau, H. Heikkinen, H. Maaheimo, A. Isogai, I. Kilpeläinen, A. W. T. King*

Materials Chemistry Division, Department of Chemistry, Faculty of Science, University of Helsinki (PO Box 55), 00014, Finland
*tetyana.koso@helsinki.fi and alistair.king@helsinki.f

The limited access to fast and facile general analytical methods for cellulosic and/or biocomposite materials currently stands as one of the main barriers for the progress of these disciplines. To that end, a diverse set of narrow analytical techniques are typically employed that often are time-consuming, costly, and/or not necessarily available on a daily basis for practitioners. Herein, we rigorously demonstrate a general quantitative NMR spectroscopic method for structural determination of crystalline cellulose samples. Our method relies on the use of a readily accessible ionic liquid electrolyte, tetrabutylphosphonium acetate ($[P_{4444}][OAc]$):DMSO- d_6 , for the direct dissolution of biopolymeric samples. We utilize a series of model compounds and apply now classical (nitroxyl-radical and periodate) oxidation reactions to cellulose samples, to allow for accurate resonance assignment, using 2D NMR. Quantitative heteronuclear single quantum correlation (HSQC) was applied in the analysis of key samples to assess its applicability as a high-resolution technique for following cellulose surface modification. Quantitation using HSQC was possible, but only after applying T2 correction to integral values. The comprehensive signal assignment of the diverse set of cellulosic species in this study constitutes a blueprint for the direct quantitative structural elucidation of crystalline lignocellulosic materials in general by readily available solution-state NMR spectroscopy.

Keywords: TEMPO, nitroxyl radical, periodate, ionic liquid, cellulose dissolution, quantitative HSQC

Table of contents

1. Materials	3
2. Methods and Analyses	3
2.1. Preparation of the [P₄₄₄₄][OAc]:DMSO-d₆ Electrolyte for NMR Analysis	3
2.2. Preparation of the Low-DP Cellulose	4
2.3. Gel Permeation Chromatography (GPC)	4
2.4. 4-AcNH-TEMPO Oxidation of the Low-DP cellulose	5
2.5. Pinnick Oxidation of Low-DP CNCs	5
2.6. Acidification of the Oxidized Low-DP Cellulose Fractions	5
2.7. Preparation of Periodate Oxidized CNCs	5
3. NMR Supplementary Data	6
3.1. NMR Sample Preparation	6
3.2. Diffusion-Edited ¹H Experiments	6
3.3. Multiplicity-Edited HSQC Experiments	6
3.4. Quantitative HSQC Experiments	6
3.5. HSQC-TOCSY Experiments	7
3.6. HMBC Experiments	7
3.7. Measurement of ¹³C Dimension Resolution in HSQC	7
3.8. Deconvolution of ¹H Spectra to Yield Number-Average Degree of Polymerizations	8
3.9. Quantitative HSQC Processing Parameters and Integration Regions	9
3.10. Glucopyranose NMR Assignment Supplementary	11
3.11. Gluconic Acid NMR Assignment Supplementary	15
3.12. Glucuronic Acid NMR Assignment Supplementary	18
3.13. Cellobiose NMR Assignment Supplementary	21
3.14. Low-DP Cellulose NMR Assignment Supplementary	24
3.15. Nitroxyl-Radical Oxidized Low-DP Cellulose NMR Assignment Supplementary	27
3.16. Cellobionic Acid NMR Assignment Supplementary	30
3.17. Reducing End Oxidation to Carboxylates NMR Assignment Supplementary	33
3.18. Periodate-Oxidized Cellulose NMR Supplementary	34
3.19. Low-DP Cellulose Structural Data	35
References	37

1. Materials

The following commercial chemicals were used in our NMR study: Microcrystalline cellulose (MCC, Avicel PH-101), D-(+)-cellobiose, D-(+)-glucose, D-(+)-gluconic acid δ -lactone, D-(+)-gluconic acid were purchased from Sigma-Aldrich (Finland). Cellobionic acid was purchased from Aldox, Department of Food Science and Technology, BOKU, Vienna, Austria.). Tri-*n*-butylphosphine (99%, Cat. # AB104493) was purchased from ABCR SWISS AG (Switzerland). Potassium acetate (98%, Cat. # 26664.293) were purchased from VWR Avantor (Finland). *n*-Chlorobutane (99%, Cat. #8.01640) was purchased from Merck Sigma-Aldrich (Finland). 4-AcNH-TEMPO (98%, Cat. #A1348) was purchased from TCI Europe (Belgium). GPC analysis standards (unbranched pullulan with DP_N = 5, 10, 20, 50, 100, 200, 400, 800) were purchased from Shodex (Showa Denko Europe GmbH, Germany). Deuterated solvent supplier is Eurisotop. All used solvents were of min. 99.9 % or HPLC purity grade.

2. Methods and Analyses

2.1. Preparation of the [P₄₄₄₄][OAc]:DMSO-*d*₆ Electrolyte for NMR Analysis

Tri-*n*-butylphosphine (35 ml, 28.7 g, 142 mmol) and *n*-butyl chloride (30 ml, 26.7 g, 288 mmol) were added sequentially and in one portion to a Teflon-lined 125 ml Parr acid digestion vessel. The vessel was sealed and its contents reacted at 120 °C for 24 h under magnetic stirring. Note: a sealed vessel is necessary as trialkylphosphines rapidly oxidize in the presence of air. Moreover, tributylphosphine is pyrophoric in air. After letting the vessel cool to room temperature, the crude and still mostly liquid product mixture was transferred to a round-bottomed flask (during this stage, rapid crystallization may occur). Excess *n*-butyl chloride (bp 78 °C) was evaporated off using a rotary evaporator. Finally, the product was dried using a high-vacuum rotary evaporator at 80 °C for 5 h, yielding a white crystalline mass (40.3 g, 137 mmol, 98% of theory); mp = 60-65 °C (from the melt); ¹H NMR (600 MHz, DMSO-*d*₆) δ 2.24 – 2.16 (m, 8H), 1.51 – 1.36 (m, 16H), 0.92 (t, *J* = 7.2 Hz, 12H). Dry [P₄₄₄₄]Cl (5.00 g, 16.96 mmol) and potassium acetate (1.67 g, 17.0 mmol) were added to isopropyl alcohol (50 ml, HPLC grade). These were mixed and refluxed with stirring for 20 h. After letting the mixture cool to room temperature and then cooling at -20 °C for 18 hr, precipitated potassium chloride was filtered off over Celite 545 and the filtrate evaporated in a rotary evaporator. Chloroform (50 ml) was added and the mixture was again cooled to -20 °C for 18 hr, to precipitate further salts, followed by filtration through Celite 545. Finally, the solvent was evaporated and the product dried in a high vacuum rotary evaporator at 90 °C for 6 h to give a pale-yellow crystalline mass (5.20 g, 16.32 mmol, 96% of theory); mp = 46 °C (from the melt); ¹H NMR (600 MHz, DMSO-*d*₆) δ 2.27 – 2.17 (m, 8H), 1.62 (s, 3H), 1.51 – 1.36 (m, 16H), 0.91 (t, *J* = 7.2 Hz, 12H). The electrolyte was prepared by weighing dry [P₄₄₄₄][OAc] into DMSO-*d*₆ in a 1:4 w/w proportion. This was stored in a sealed vessel to avoid water uptake. The sample was analyzed by NMR to assess purity (Fig. S1).

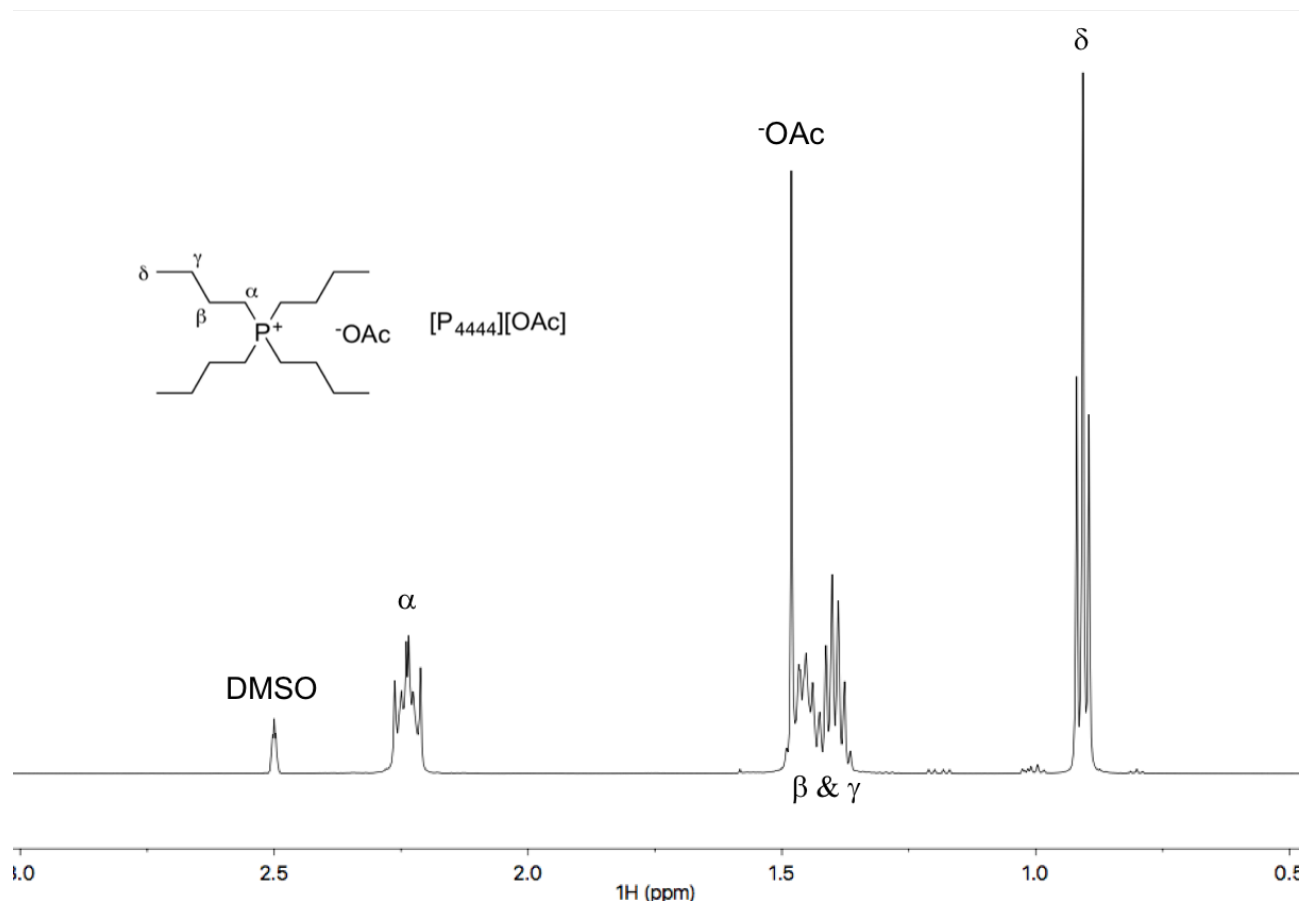


Figure S1 ^1H NMR of the prepared $[\text{P}_{4444}][\text{OAc}]:\text{DMSO-}d_6$ electrolyte

2.2. Preparation of the Low-DP Cellulose

Low DP cellulose nanocrystals (LDP-CNCs) was prepared by sc- H_2O extraction of MCC, as described previously using a plug-flow reactor (Buffiere et al. 2016; Tolonen et al. 2013). Briefly, A 1.0 wt% MCC suspension was pressurized and mixed with a preheated supercritical water stream with a ratio of 2:3 at the one end of a tubular reactor (diameter 3 mm, length 55 mm). Mass-flow rates were set to allow for 0.4 s residence time at 375 °C and 25 MPa in the reactor. The reaction was stopped by quenching with a cold-water flow at the other end of the reactor down to a subcritical temperature of 268 °C, after which the product was further cooled down using a cold-water jacket and depressurized to atmospheric pressure for sample collection. Immediately after cooling, the residual suspended solids were separated by ultracentrifugation (Eppendorf model 5804 R, Hamburg, Germany) at 10000 rpm for 30 min. These were isolated as a 15 wt% paste and stored in the freezer to prevent mold formation.

2.3. Gel Permeation Chromatography (GPC)

17.5 mg of cellulosic material were weighted into glass vial, DMAc (1.25 mL) was added and suspension was stirred at 130°C for 2 h. Then sample was allowed to cool to 90°C and 87.5 mg of anhydrous LiCl were added. Sample was further stirred overnight at ambient temperature. Further, sample was diluted with 16.23 mL of DMAc so that final concentration of LiCl in the solution would be 0.5 w/v % and additionally stirred for 1 h. Before the injection all the samples were also filtered through Pall Acrodisc GHP 0.45 μm filters.

2.4. 4-AcNH-TEMPO Oxidation of the Low-DP cellulose

The cellulosic sample (250 mg, 1.54 mmol) was dispersed into 25 mL of 0.1 M acetate buffer (pH 5.80) in a round-bottomed flask, equipped with a magnetic stirrer bar. To this suspension, NaClO₂ (80%, 212 mg, 1.87 mmol) and 4-AcNH-TEMPO (24 mg, 0.112 mmol) were added, followed by NaClO (aq., 10%, 0.08 mL, 0.125 mmol), additionally diluted to concentration of ca. 1% with distilled water. The reaction mixture was stirred in the sealed flask at 40°C for 24 h. Additional portions of NaClO₂ (80%, 212 mg, 1.87 mmol) and NaClO (aq., 10%, 0.08 mL, 0.125 mmol, diluted to 1%) were added and the reaction mixture was stirred at 40°C for an additional 48 h (Hirota et al. 2009). After the reaction time was complete, a solid precipitate was separated by centrifugation and subsequently washed with distilled water (3 × 30 mL) and ethanol (3 × 25 mL), with parallel collection of the supernatants. The supernatant, which contained the water-soluble fraction of the oxidized LDP-CNCs, was diluted additionally with ethanol (ca. 100 mL), and further centrifuged to collect the precipitated solids. The obtained water soluble and insoluble fractions of the oxidized celluloses, in the form of sodium salts, were finally freeze-dried.

2.5. Pinnick Oxidation of Low-DP CNCs

NaClO₂ (16.5 mg) in 1.6 ml of sodium acetate buffer solution (0.2 M, pH = 5.0) was added to the freeze-dried LDP-CNCs (50 mg) in an 8 ml vial. The vial was sealed and reaction mixture was stirred at 40 °C. After 2 hr, another portion of NaClO₂ (16.5 mg in 1.6 ml of acetate buffer) was added and the reaction mixture was stirred at 40 °C for a further 18 hr. After this, the last portion of NaClO₂ (16.5 mg in 1.6 ml of acetate buffer) was added and the reaction mixture was stirred at 40 °C for 4 more hr (total 24 h at 40 °C). The reaction mixture was cooled and washed/centrifuged with H₂O (2 x 5 ml) and EtOH (3 x 5 ml). The recovered solid was then freeze-dried. This sample was then acidified in accordance with procedure (Fujisawa et al. 2010, Section 2.5.1) and solid was washed/centrifuged with H₂O (2 x 5 ml), before freeze-drying.

2.6. Acidification of the Oxidized Low-DP Cellulose Fractions

Sodium carboxylates of oxidized LDP-CNCs (as obtained) were found to be partially or non-soluble in the [P₄₄₄₄][OAc]:DMSO-d₆ electrolyte. The materials were acidified according to a previous article (Fujisawa et al. 2010): To 2 w/v % of oxidized cellulosic material suspension in water (100 mg in 5 mL of water), 0.2 M HCl (aq., 5 mL) was added to give a 1 w/v % suspension, with a pH ca. 1.0. The white precipitates were separated by centrifugation and further washed/centrifuged with water (3 × 10 mL), before freeze-drying.

2.7. Preparation of Periodate Oxidized CNCs

The pristine CNCs were prepared according to a previous publication (Nypelö et al. 2018) from cotton that was a donation from USDA (United States Department of Agriculture, New Orleans Research Center). Hydrolysis was performed using 65 wt % H₂SO₄ (prepared from 95–97% purity, Sigma-Aldrich) for 30 min followed by purification through centrifugation and dialysis. The CNCs were desulphated in 2.5 M hydrochloric acid (prepared from 37% reagent grade, Sigma-Aldrich) at 90 °C for 180 min, followed by dialysis. The periodate-oxidized CNCs (NaIO₄-CNC) were then prepared by addition of sodium periodate (9.2 g, 43.01 mmol, purity 99.5%, Sigma-Aldrich) dissolved in 500 mL of deionized water (purified using Milli-Q water purification system) to 1500 mL of nanocrystalline cellulose aqueous suspension (0.42 wt %). The mixture was stirred for 176 h in the absence of light at room temperature and the progress of the reaction was followed using ultraviolet (UV) spectroscopy (Lambda 35 by PerkinElmer) to measure the absorption of the supernatant at 290 nm. Residual sodium periodate was then quenched using glycerol (purity 99.5%, Sigma-Aldrich) and the product was dialyzed against deionized water for 7 days with a molecular weight cutoff of

12–14 kDa. An aqueous suspension of ca. 1 wt% concentration was cast as a film on a polystyrene petri dishes and left to evaporate at room temperature and was finally stored in a desiccator prior to NMR analysis.

3. NMR Supplementary Data

3.1. NMR Sample Preparation

To prepare the samples for NMR analysis, typically 50 mg of dried sample is added to a sealable sample vial and made up to 1 g, by addition of stock [P₄₄₄₄][OAc]:DMSO-d₆ (20:80 wt%) electrolyte solution (King et al. 2018). The samples were magnetically stirred at RT until they go clear. This typically was over a 1 hr period. If the samples did not go clear during that period, the temperature was typically increased to 60 °C. All further NMR experiments were recorded on a Bruker AVANCE NEO 600 MHz spectrometer equipped with a 5 mm SmartProbe™.

3.2. Diffusion-Edited ¹H Experiments

The diffusion-edited ¹H experiment used a 1D bipolar-pulse pair with stimulated echo (BPPSTE) (Wu et al. 1995) diffusion-ordered spectroscopy (DOSY) pulse sequence (Bruker pulse program 'ledbpgp2s1d'), with 1 s relaxation delay (d1), 0.5 s acquisition time (aq), 16 dummy scans (ds) and 512 transient scans (ns), a sweep-width (sw) of 20 ppm with the transmitter offset on 6.1 ppm (o1p), a diffusion time (d20) of 200 ms, a gradient recovery delay (d16) of 0.2 ms, an eddy current delay (d21) of 5 ms, , a diffusion gradient pulse duration (p30) of 2.5 ms and a z-gradient strength (gpz6) of 90% at ≥ 50 G/cm (probe z-gradient strength). These conditions are specific to the Bruker AVANCE NEO 600 MHz - SmartProbe™ system.

3.3. Multiplicity-Edited HSQC Experiments

The HSQC experiments on cellulose samples used either a multiplicity-edited phase sensitive HSQC sequence with echo/antiecho-TPPI gradient selection (Bruker pulse program 'hsqcedetgp') (Willker et al. 1993) or a sensitivity improved multiplicity-edited phase sensitive HSQC sequence with echo/antiecho-TPPI gradient selection and adiabatic pulses (Bruker pulse program 'hsqcedetgpsisp2.2'), for increased sensitivity (Willker et al. 1993; Palmer III et al. 1991; Kay et al. 1992; Schleucher et al. 1994). Typical parameters are as follows: spectral widths (sw) were 13.03 and 165 ppm, with transmitter offsets (o1p) of 6.18 and 75 ppm, for ¹H and ¹³C dimensions, respectively. The time-domain size (td1) in the indirectly detected ¹³C-dimension (f1) was 512 or 1024, corresponding to 256 or 512 t₁-increments for the real spectrum. There were 16 dummy scans (ds), typically 8 (or multiples of 8) scans (ns), an acquisition time (aq) of 0.065 s for f2 and a relaxation delay of 1.5 s. If samples were of sufficient signal-to-noise, spectral resolution was increased by zero-filling, typically by doubling or quadrupling the spectrum size in f1, e.g. 512 to 1024 or 2048 Hz. Window functions were typically sine squared (90 °) in f1 and f2.

3.4. Quantitative HSQC Experiments

The following experiments were run both on a Bruker 600 MHz Avance III with a cryogenically He-cooled (QCI) probe-head (¹H, ¹³C, ³¹P, ¹⁴N) with z-gradients and a Bruker 600 MHz Neo with a triple resonance inverse (TXI) probe-head (¹H/¹⁹F, ¹³C, ³¹P) with xyz-gradients. Quantitative Carr-Purcell-Meiboom-Gill (CPMG)-adjusted HSQC (Q-CAHSQC) experiments (Koskela et al. 2005) were recorded for the LDP-CNC, TOx-LDP-CNC and MCC samples. The sequence ('qcahsqc') was obtained directly from Bruker. Typical parameters are as follows: spectral widths (sw) were 6.0 and 120 ppm, with transmitter offsets (o1p) of 3.0 and 60 ppm, for ¹H

and ^{13}C dimensions, respectively. The time-domain size (td1) in the indirectly detected ^{13}C -dimension (f1) was 64, 256 or 320, corresponding to 128, 512 or 640 t_1 -increments for the real spectrum. There were 16 dummy scans (ds), typically 8 (or multiples of 8) scans (ns), an acquisition time (aq) of 0.065 s for f2 and a relaxation delay of 12.5 s. Window functions were typically sine squared (90°) in f1 and f2, with no linear prediction.

3.5. HSQC-TOCSY Experiments

The HSQC-TOCSY experiments on cellulose samples used a phase sensitive HSQC-TOCSY pulse program with the DIPSI-2 isotropic mixing sequence and echo/antiecho-TPPI gradient selection (Bruker pulse program 'hsqcdietgpsisp.2') (Willker et al. 1993). Typical parameters are as follows: spectral widths (sw) were 13.0 and 200 ppm, with transmitter offsets (o1p) of 6.18 and 90 ppm for ^1H and ^{13}C dimensions, respectively. The time-domain size (td1) was 512 or 1024 in the indirectly detected ^{13}C -dimension (f1) dimension. There were 16 dummy scans (ds), typically 8 (or multiples of 8) scans (ns), an acquisition time (aq) of 0.107 s for f2 and a relaxation delay of 1.5 s. The TOCSY mixing delay (d9) was 0.015 s to yield a short-range (COSY-like) TOCSY experiment or 0.12 s to yield a long-range TOCSY experiment, where the full spin-system was typically observed. The latter experiment required typically 2-4 times the scans (ns) to get similar signal-to-noise as the short-range experiment. If samples were of sufficient signal-to-noise, spectral resolution was increased by zero-filling, typically by doubling or quadrupling the spectrum size in f1, e.g. 512 to 1024 or 2048 Hz. Window functions were typically sine squared (90°) in f1 and f2.

3.6. HMBC Experiments

The HMBC experiment for the cellulose samples used a magnitude-mode gradient-enhanced HMBC sequence using a low-pass J -filter (Bax & Summers 1986) (Bruker pulse program 'hmbcgpplndqf'). Spectral widths (sw) were 13.0 and 250 ppm, with transmitter offsets (o1p) of 6.3 and 100 ppm for ^1H and ^{13}C dimensions, respectively. The time-domain size (td1) in the indirectly detected ^{13}C -dimension (f1) was 512. For magnitude mode HMBC this directly corresponds to 512 t_1 -increments for the real spectrum. There were 16 dummy scans (ds), 32 scans (ns), an acquisition time (aq) of 0.131 s for f2 and a relaxation delay of 1.5 s. A $^1J_{\text{CH}}$ coupling constant value (cnst2) of 145 Hz was used, for setting up the low-pass filter. The polarization transfer delay was optimized for a $^nJ_{\text{CH}}$ long-range coupling constant value of 10 Hz (cnst13). If samples were of sufficient signal-to-noise, spectral resolution was increased by zero-filling, typically by doubling or quadrupling the spectrum size in f1, e.g. 512 to 1024 or 2048 Hz. Window functions were typically sine bell (0°) in f1 and f2.

3.7. Measurement of ^{13}C Dimension Resolution in HSQC

HSQC experiments on MCC (Bruker pulse program 'hsqcedetgp') (Willker et al. 1993) were recorded, with increasing td1 values (real and imaginary f1 increments). The ^{13}C projections were extracted and deconvoluted with Gaussian peaks, in Topspin 4.0.6. The full-width at half-maximum (FWHM) values were plotted against the number of t_1 -increments (td1/2) (Fig. S2).

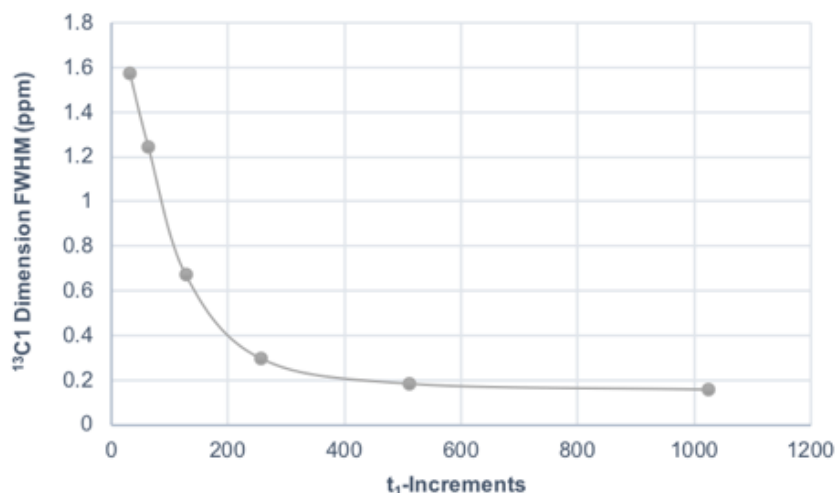


Figure S2 Resolution in the ¹³C dimension of HSQCs for C1 in MCC (DP_N 153), with increasing number of real t₁-increments, as measured by the full-width at half-maximum (FWHM) values (in ppm) of the CH1 correlation 1D projections. The plotted t₁-increment values correspond to digital f1-resolutions of 778, 389, 194, 97, 49 and 24 Hz/pt

3.8. Deconvolution of ¹H Spectra to Yield Number-Average Degree of Polymerizations

Quantitative ¹H spectra for MCC and LDP-CNCs were recorded with a 10 s relaxation delay (30 ° pulse) and 16 transients collected. The spectra were calibrated and phased using Topspin 4.0.6 The region from 4-5 ppm was output as a comma-separated value (.csv) file, from MestreNova 10.0. This was then opened in 'Fityk 1.3.1'. with the '.xy' file ending. The data was then baseline corrected using spline baseline correction (Fig. S3a & c). Gaussian functions were then applied representing the polymeric H1 (AGU-1), non-reducing end H1 (NRE-1), reducing end alpha H1 (α-RE-1) and reducing end beta H1 (β-RE-1) resonances (Fig. S3b & d). The β-RE-1 signal was not separable from the anhydroxylose unit H1 (AXU-1) signal in MCC, so was disregarded. The DP_{N-¹H} values were then calculated by division of the overall peak volume by the values obtained from the NRE or RE signals, according to the equation 1. In the case of MCC the value for RE-1 was taken to be (2.94 × β-RE-1), based on the integral ratio of (β-RE-1/α-RE-1) from cellobiose. Thus, the DP_{N-¹H} was calculated according to equation 2.

$$DP_{N-^1H} = \frac{\alpha-RE-1 + \beta-RE-1 + NRE + AGU-1}{\alpha-RE-1 + \beta-RE-1} \quad (\text{equation 1})$$

$$DP_{N-^1H} = \frac{\alpha-RE-1 + \beta-RE-1 + NRE + AGU-1}{2.94 \times \alpha-RE-1} \quad (\text{equation 2})$$

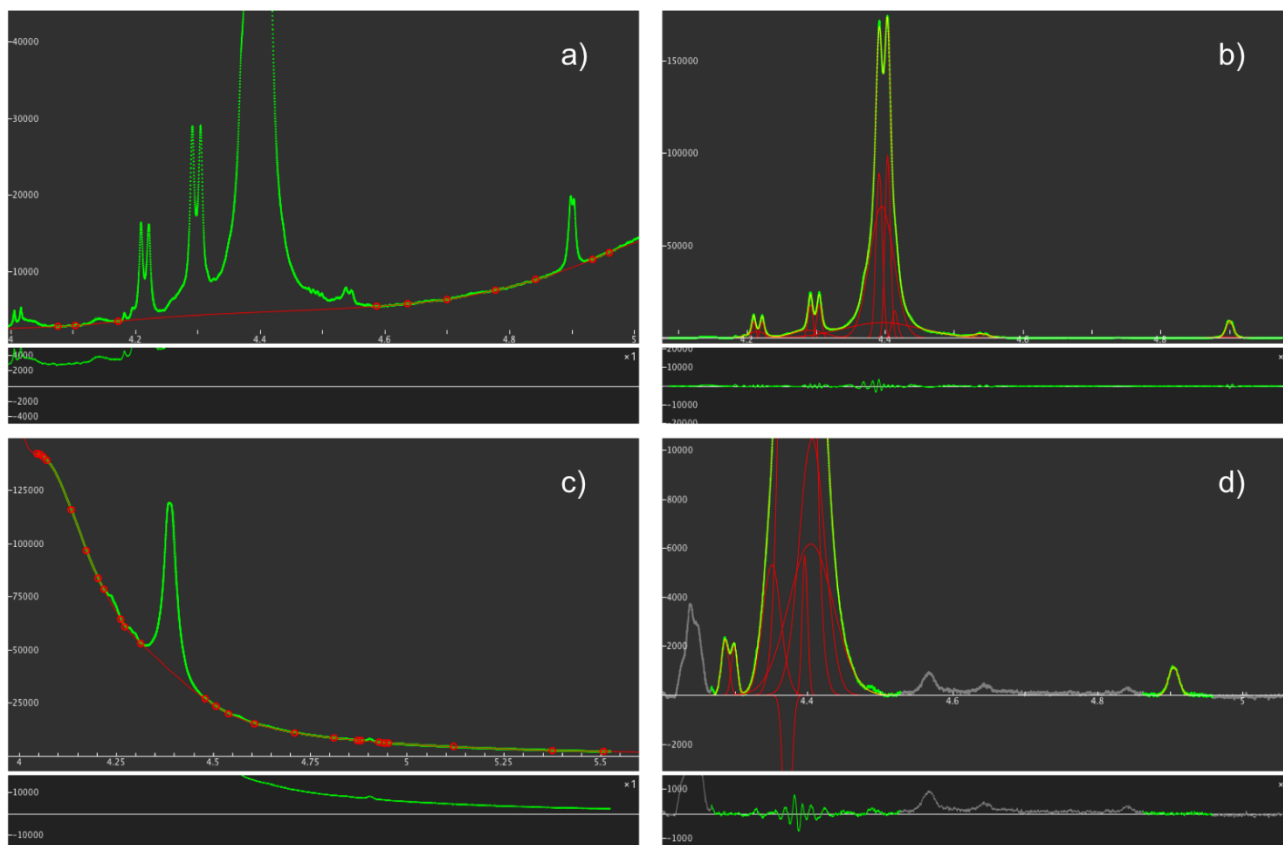


Figure S3 Deconvolution of quantitative ^1H cellulose H1 regions using *Fityk* 1.3.1: a) spline baseline correction for LDP-CNC, b) Gaussian deconvolution for LDP-CNC, c) spline baseline correction for MCC, d) Gaussian deconvolution for MCC

In the case of the LDP-CNCs an average value of 15 was calculated for $\text{DP}_{\text{N-}^1\text{H}}$, based on an average of the values derived from the RE (17.4) vs NRE (11.8) signals.

3.9. Quantitative HSQC Processing Parameters and Integration Regions

Quantitative 2D HSQC spectra were initially phased in Topspin 4.0. The spectra were further opened in MestreNova 10.0 and baseline corrected in both dimensions using a 3rd order polynomial. There was no linear prediction used. The integral regions are shown in Fig. S4.

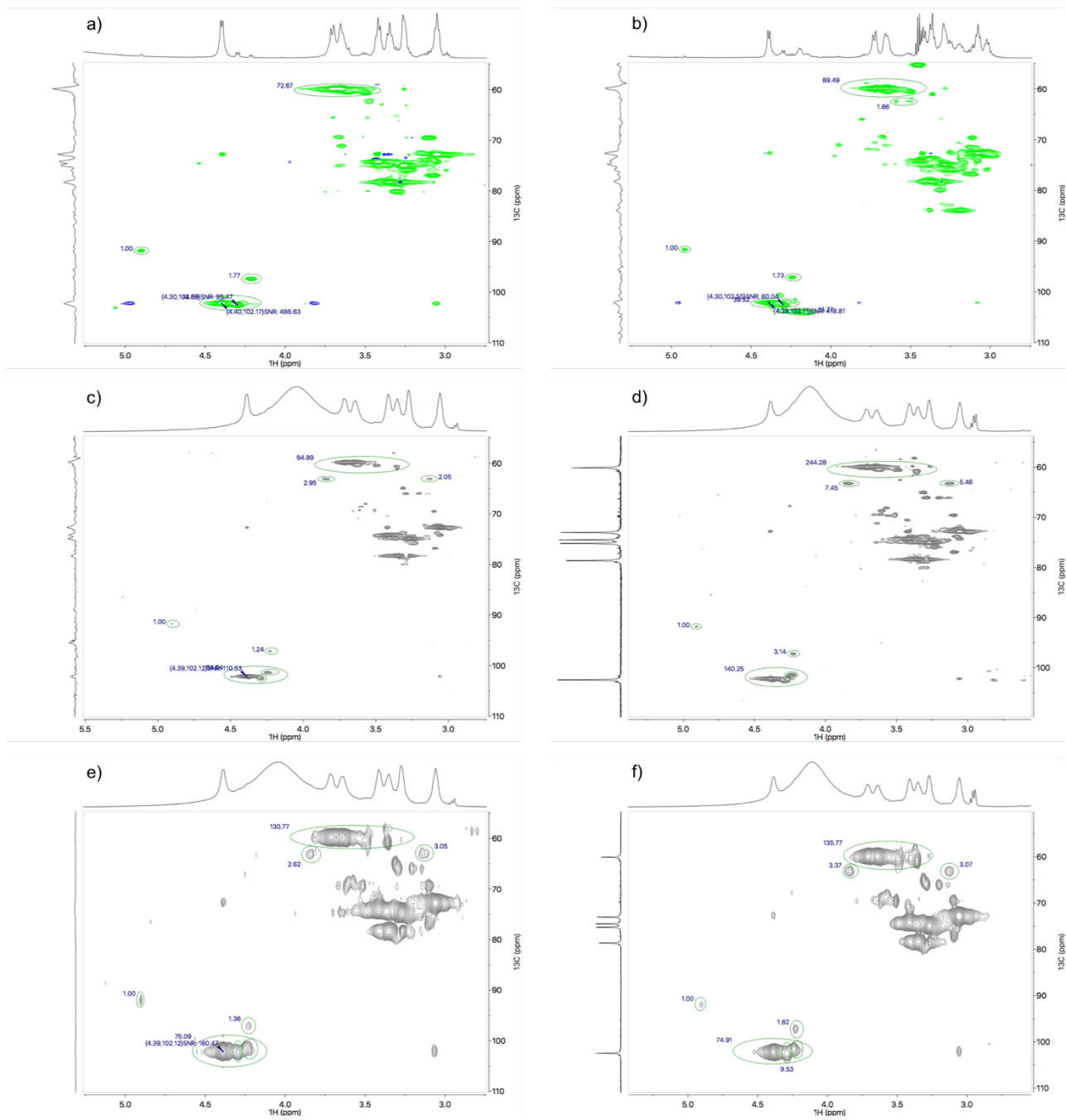


Figure S4 2D HSQC Integral regions for: a) LDP-CNCs, b) TOx-LDP-CNCs, c) MCC (td1 = 640, ns = 8, RT probe-head), d) MCC (td1 = 640, ns = 8, cryoprobe-head), e) MCC (td1 = 128, ns = 40, RT probe-head), and e) MCC (td1 = 128, ns = 40, cryoprobe-head)

3.10. Glucopyranose NMR Assignment Supplementary

Table S1 Full peak assignment of α - and β -D-glucopyranose (α - and β -D-Glcp) referenced to [P₄₄₄₄][OAc]:DMSO-d₆ (20:80, ¹H: δ = 2.50 ppm, ¹³C: δ = 39.52 ppm) and to D₂O at 30 °C (¹H: δ = 4.79 ppm, *italics*, Roslund et al. 2008)

α -D-Glcp	¹ H, ppm	¹ H, ppm	¹³ C, ppm	¹³ C, ppm	β -D-Glcp	¹ H, ppm	¹ H, ppm	¹³ C, ppm	¹³ C, ppm
1	4.90(d) J = 3.7 Hz	5.21 J = 3.8 Hz	92.16	92.77	1	4.19 (d) J = 7.7 Hz	4.63 J = 8.0 Hz	97.64	96.59
2	3.11 (m)	3.52	72.88	72.15	2	2.98 (m)	3.23	74.34	74.81
3	3.54 (m)	3.70	72.81	73.43	3	3.11 (m)	3.47	76.40	76.43
4	3.11 (m)	3.39	70.86	70.32	4	3.11 (m)	3.38	70.76	70.27
5	3.54 (m)	3.82	71.56	72.10	5	2.98 (m)	3.45	76.62	76.61
6	3.54 (m)	3.82; 3.74	61.36	61.27	6	3.54 (m)	3.88; 3.70	61.36	61.42

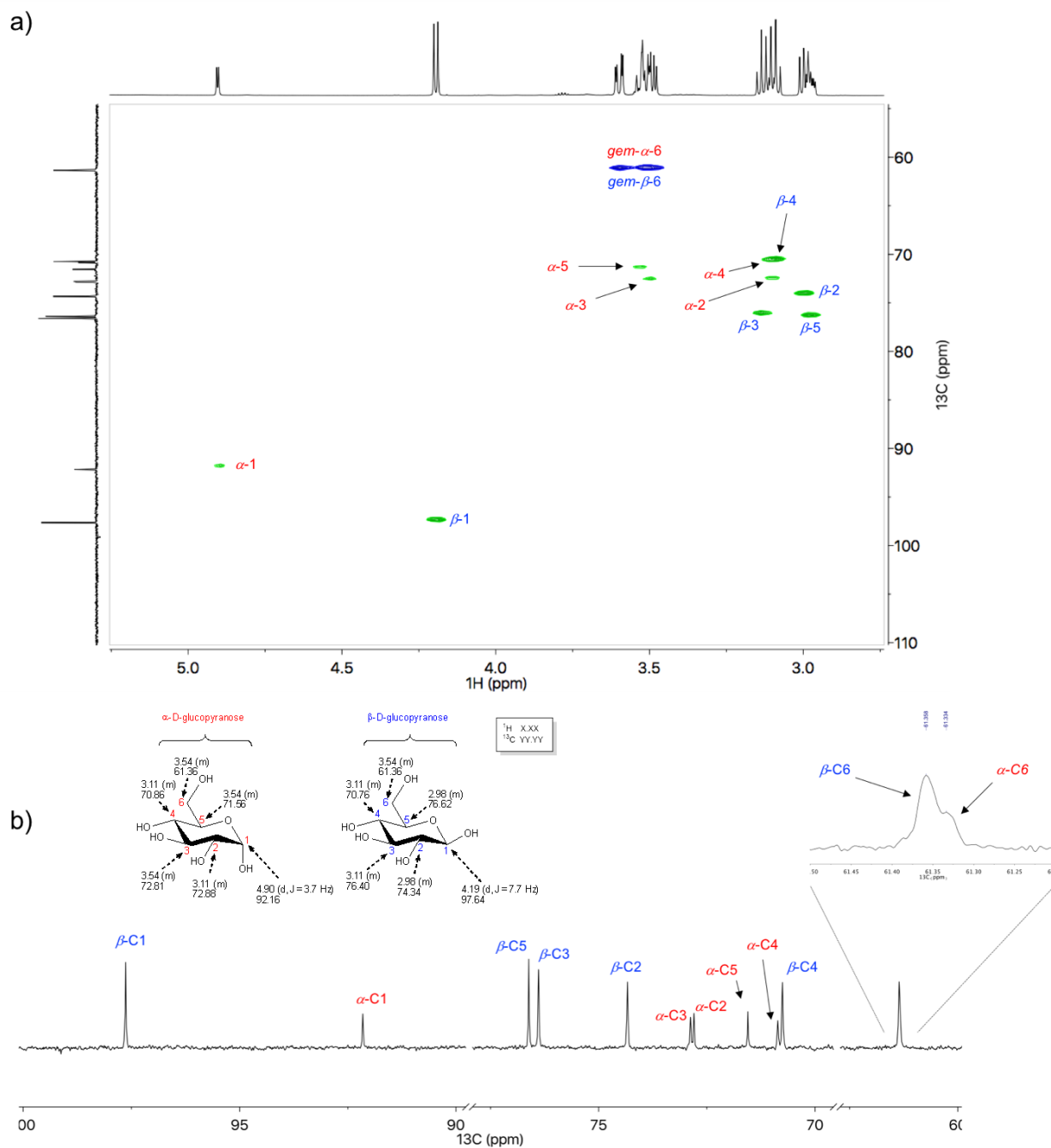


Figure S5 Glucose spectra at 65 °C in $[\text{P}_{4444}][\text{OAc}]:\text{DMSO-d}_6$ (5 wt %): (a) Multiplicity-edited 2D HSQC (1024 time-domain data size in f_1 , corresponding to 512 actual t_1 -increments); (b) ^{13}C Spectrum. α and β anomeric resonances color coded with red and blue, respectively

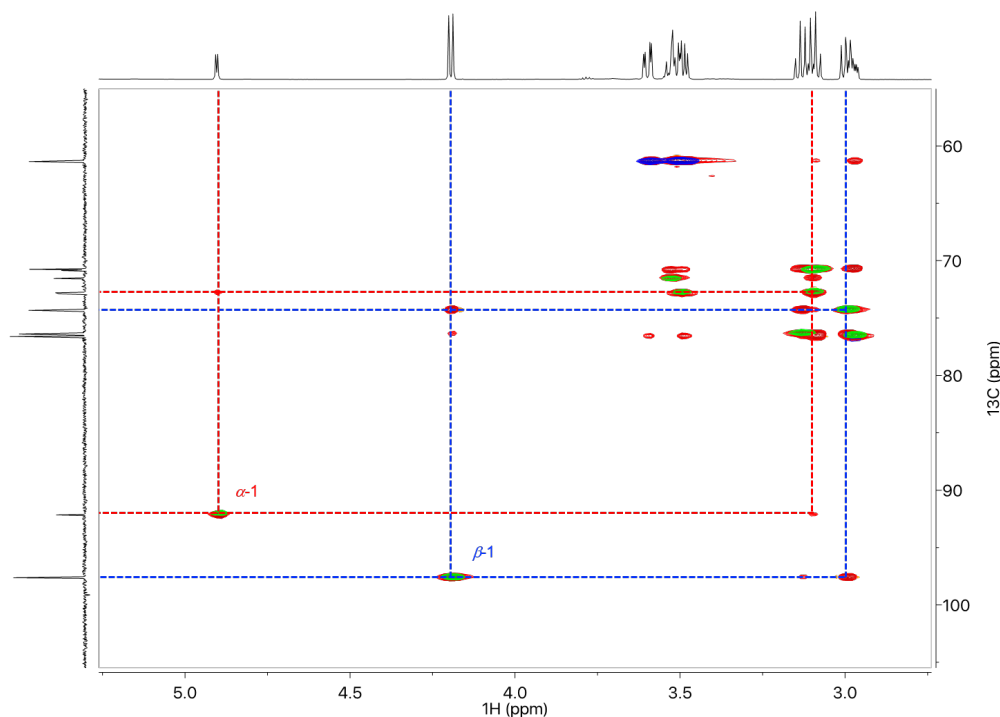


Figure S6 Glucose spectra at 65 °C in [P₄₄₄₄][OAc]:DMSO-d₆ (5 wt %): overlay of the multiplicity-edited 2D HSQC (1024 time-domain data size in f1, corresponding to 512 actual t₁-increments) and HSQC-TOCSY (15ms) with CH1-CH2 correlations of α (red) and β (blue) anomers. Overlay spectrum cross-peaks are blue/green for HSQC layer and red for HSQC-TOCSY

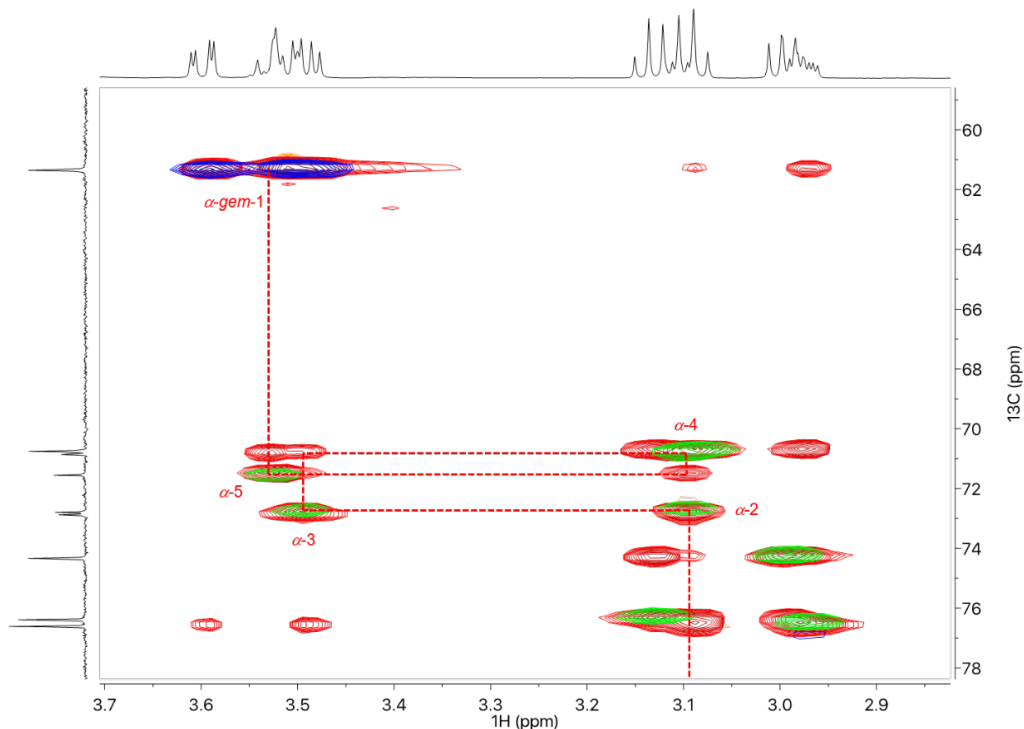


Figure S7 Glucose spectra at 65 °C in [P₄₄₄₄][OAc]:DMSO-d₆ (5 wt %): overlay of the multiplicity-edited 2D HSQC (1024 time-domain data size in f1, corresponding to 512 actual t₁-increments) and HSQC-TOCSY (15ms) with CH2-CH6 correlations of α (red) anomers. Overlay spectrum cross-peaks are blue/green for HSQC layer and red for HSQC-TOCSY

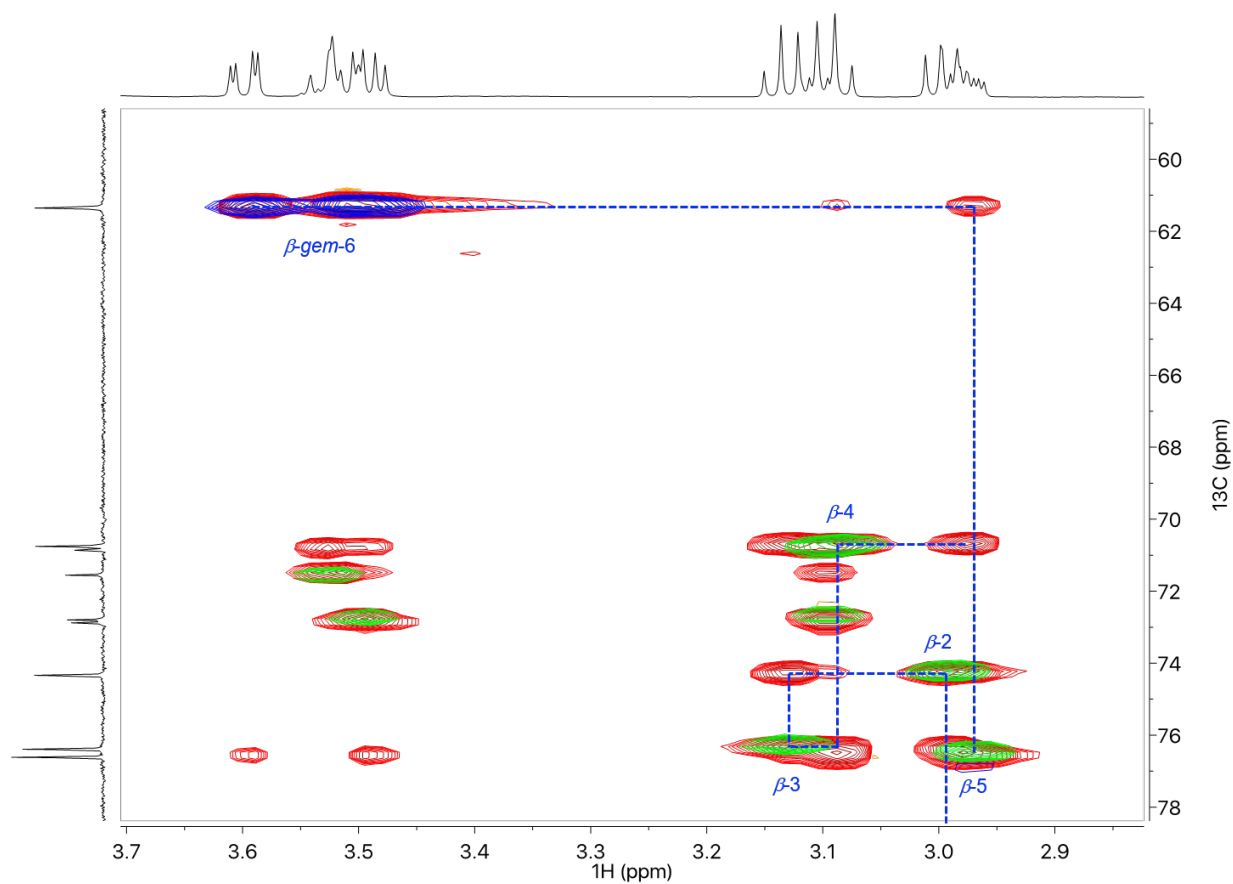


Figure S8 Glucose spectra at 65 °C in [P₄₄₄₄][OAc]:DMSO-d₆ (5 wt %): overlay of the multiplicity-edited 2D HSQC (1024 time-domain data size in f1, corresponding to 512 actual t₁-increments) and HSQC-TOCSY (15ms) with CH₂-CH₆ correlations of β (blue) anomers. Overlay spectrum cross-peaks are blue/green for HSQC layer and red for HSQC-TOCSY

3.11. Gluconic Acid NMR Assignment Supplementary

Table S2 Full peak assignment of gluconic acid (GI-COOH) and its δ -gluconolactone (GI-lact) referenced to [P₄₄₄₄][OAc]:DMSO-d₆ (20:80, ¹H: δ = 2.50 ppm, ¹³C: δ = 39.52 ppm)

GI-COOH	¹ H, ppm	¹³ C, ppm	GI-lact	¹ H, ppm	¹³ C, ppm
1	-	175.66	1	-	175.15
2	4.02 (d) J = 3.3 Hz	73.45	2	3.48 (m)	72.48
3	4.19 (dd) J = 4.3; 3.4 Hz	72.71	3	3.78 (dd) J = 4.9; 2.3 Hz	71.00
4	4.36 (dd) J = 7.5; 4.4 Hz	80.73	4	3.48 (m)	72.17
5	3.81 (ddd) J = 7.6; 5.7; 3.4 Hz	68.73	5	3.48 (m)	71.69
6	3.48 (m)	62.92	6	3.48 (m)	63.72

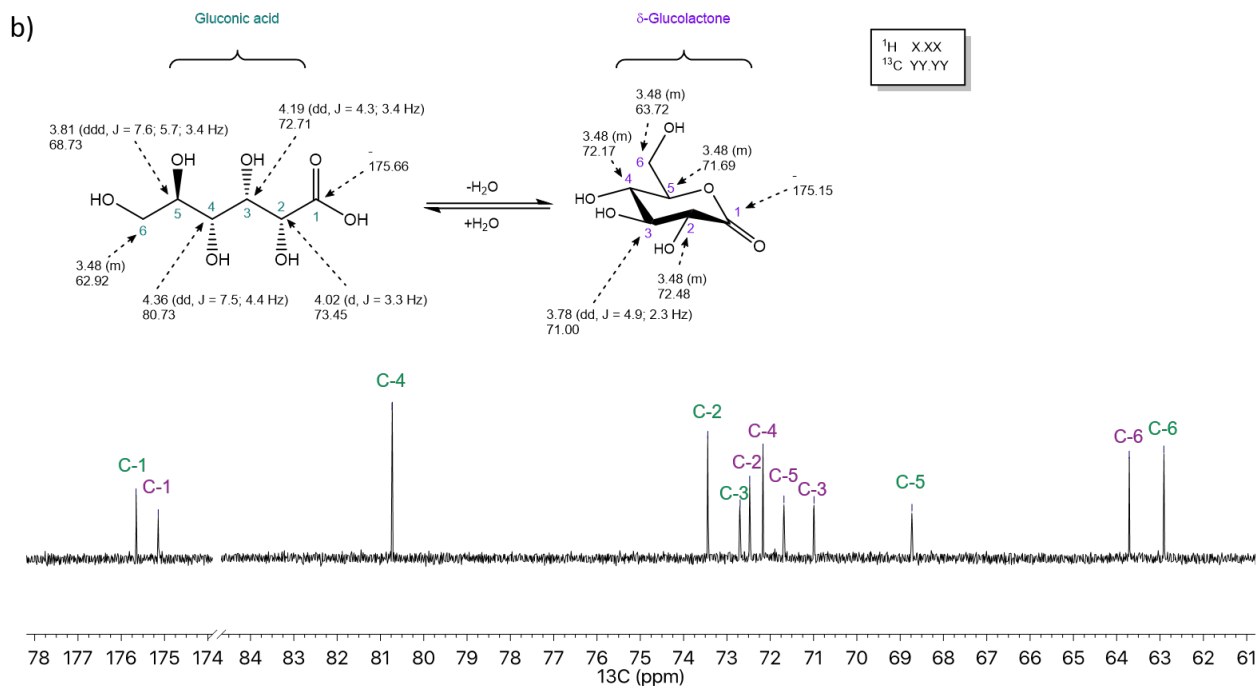
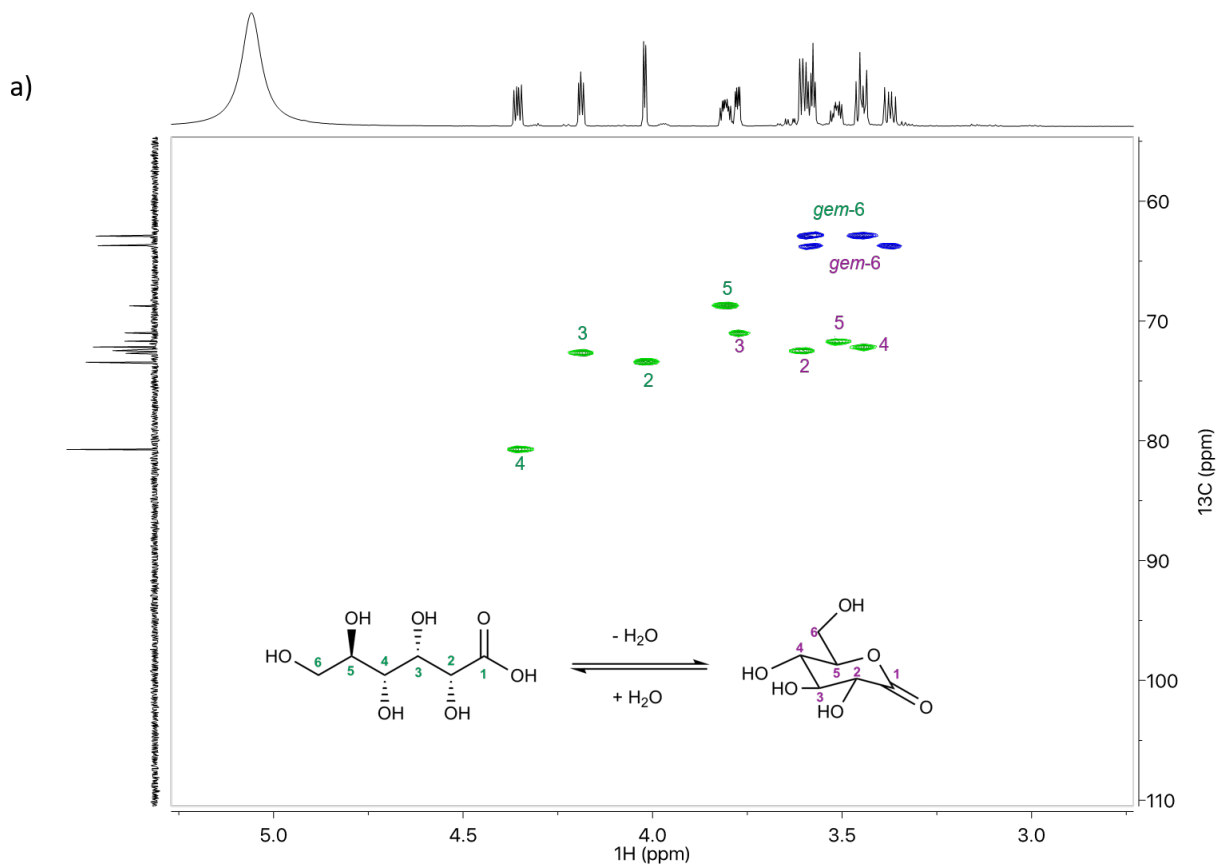


Figure S9 Dry gluconic acid spectra at 65 °C in [P₄₄₄₄][OAc]:DMSO-d₆ (5 wt %): (a) Multiplicity-edited 2D HSQC (1024 time-domain data size in f1, corresponding to 512 actual t₁-increments); (b) refocused INEPT. The spectra clearly show two spin-systems, corresponding to gluconic acid (turquoise) and δ -gluconolactone (purple)

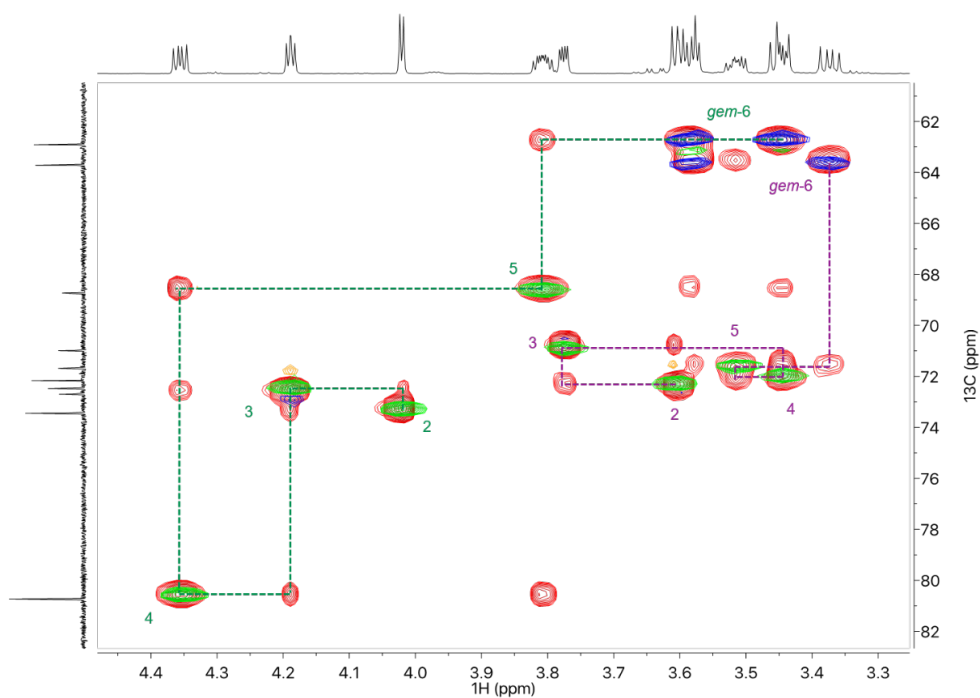


Figure S10 Gluconic acid spectra at 65 °C in [P₄₄₄₄][OAc]:DMSO-d₆ (5 wt %): overlay of the multiplicity-edited 2D HSQC (1024 time-domain data size in f1, corresponding to 512 actual t₁-increments) and HSQC-TOCSY (15ms) with CH1-CH6 correlations of gluconic acid (turquoise) and δ -gluconolactone (purple). Overlay spectrum cross-peaks are blue/green for HSQC layer and red for HSQC-TOCSY

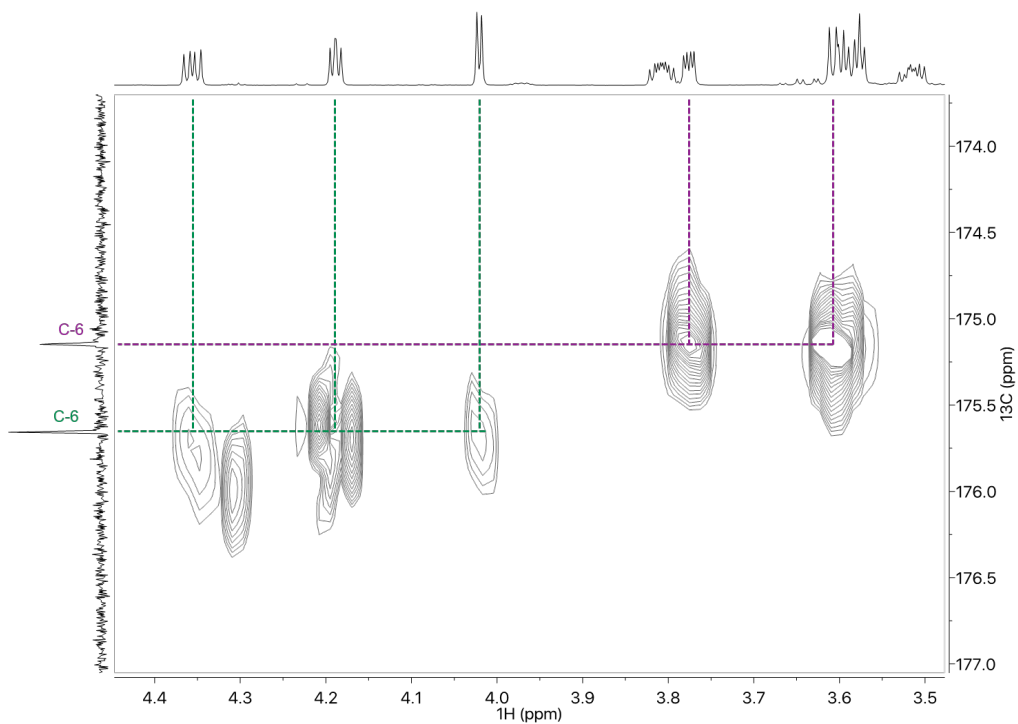


Figure S11 Gluconic acid spectra at 65 °C in [P₄₄₄₄][OAc]:DMSO-d₆ (5 wt %): 2D HMBC (512 time-domain data size in f1, also corresponding here to 512 actual t₁-increments) – C6 related correlations of gluconic acid (turquoise) and δ -gluconolactone (purple)

3.12. Glucuronic Acid NMR Assignment Supplementary

The glucuronic acid spectral data was recorded using DMSO-d₆ as the perdeuterated solvent as the [P₄₄₄₄][OAc]:DMSO-d₆ electrolyte rapidly decomposed the sample.

Table S3 Full peak assignment of glucuronic acid (α - and β -Glc_{ur}-COOH) referenced to DMSO-d₆ (20:80, ¹H: δ = 2.50 ppm, ¹³C: δ = 39.52 ppm) and its sodium salt in D₂O/acetone at 25 °C (¹H: δ = 2.225 ppm, *italics*, Agrawal 1992)

α -Glc _{ur} -COOH	¹ H, ppm	¹ H, ppm	¹³ C, ppm	¹³ C, ppm	β -Glc _{ur} -COOH	¹ H, ppm	¹ H, ppm	¹³ C, ppm	¹³ C, ppm
1	4.93 (m)	5.25	92.90	93.0	1	4.33 (d) J = 6.7 Hz	4.65	97.43	96.8
2	3.16 (dd) J = 9.7; 3.2 Hz	3.59	72.04	72.3	2	2.93 (t) J = 8.5 Hz	3.30	74.56	75.0
3	3.41 (t) J = 9.1 Hz	3.75	72.71	73.5	3	3.13 (t) J = 9.0 Hz	3.52	76.09	76.5
4	3.29 (t) J = 9.2 Hz	3.53	72.04	72.9	4	3.30 (t) J = 9.2 Hz	3.54	71.63	72.7
5	3.98 (d) J = 9.8 Hz	4.09	71.48	72.5	5	3.57 (d) J = 9.7 Hz	3.72	75.77	76.9
6	-	-	171.46	177.4	6	-	-	170.57	176.5

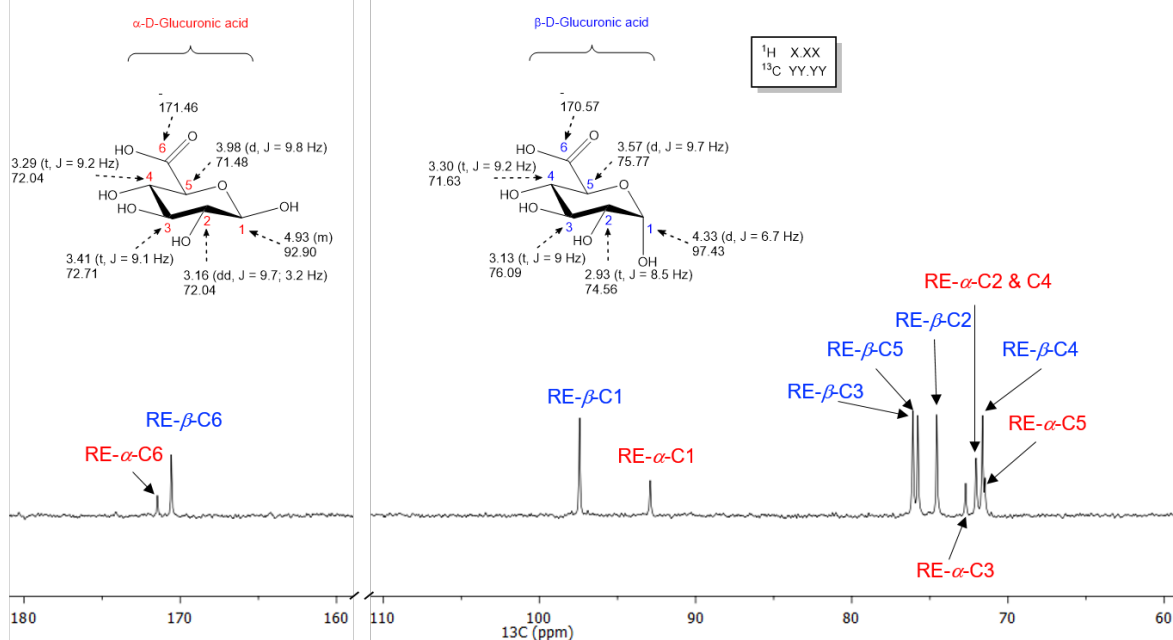
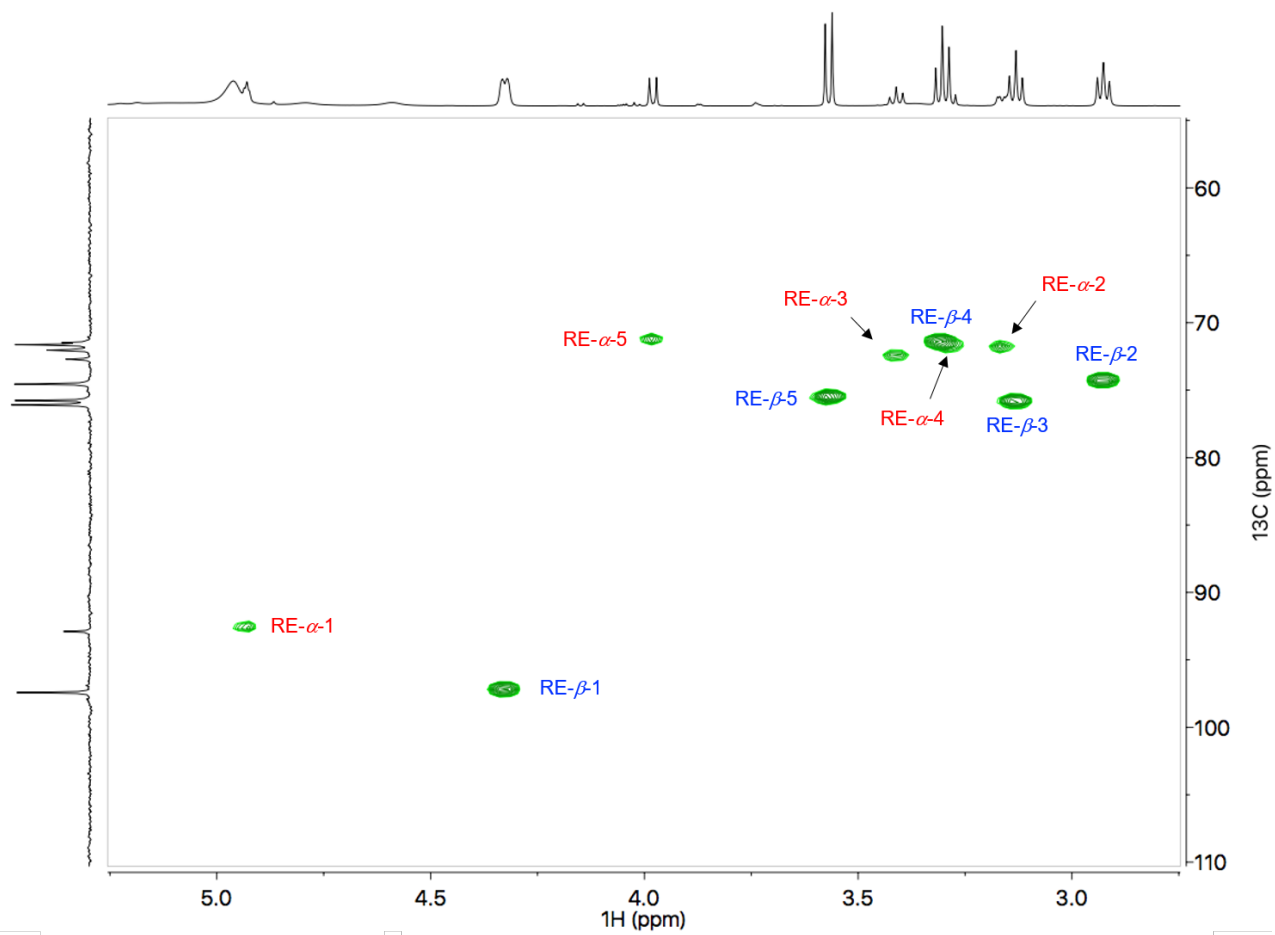


Figure S12 Glucuronic acid spectra at 65 °C in DMSO- d_6 (5 wt %): (a) Multiplicity-edited 2D HSQC (1024 time-domain data size in f1, corresponding to 512 actual t_1 -increments); (b) ^{13}C experiment. α and β anomeric resonances color coded with red and blue, respectively

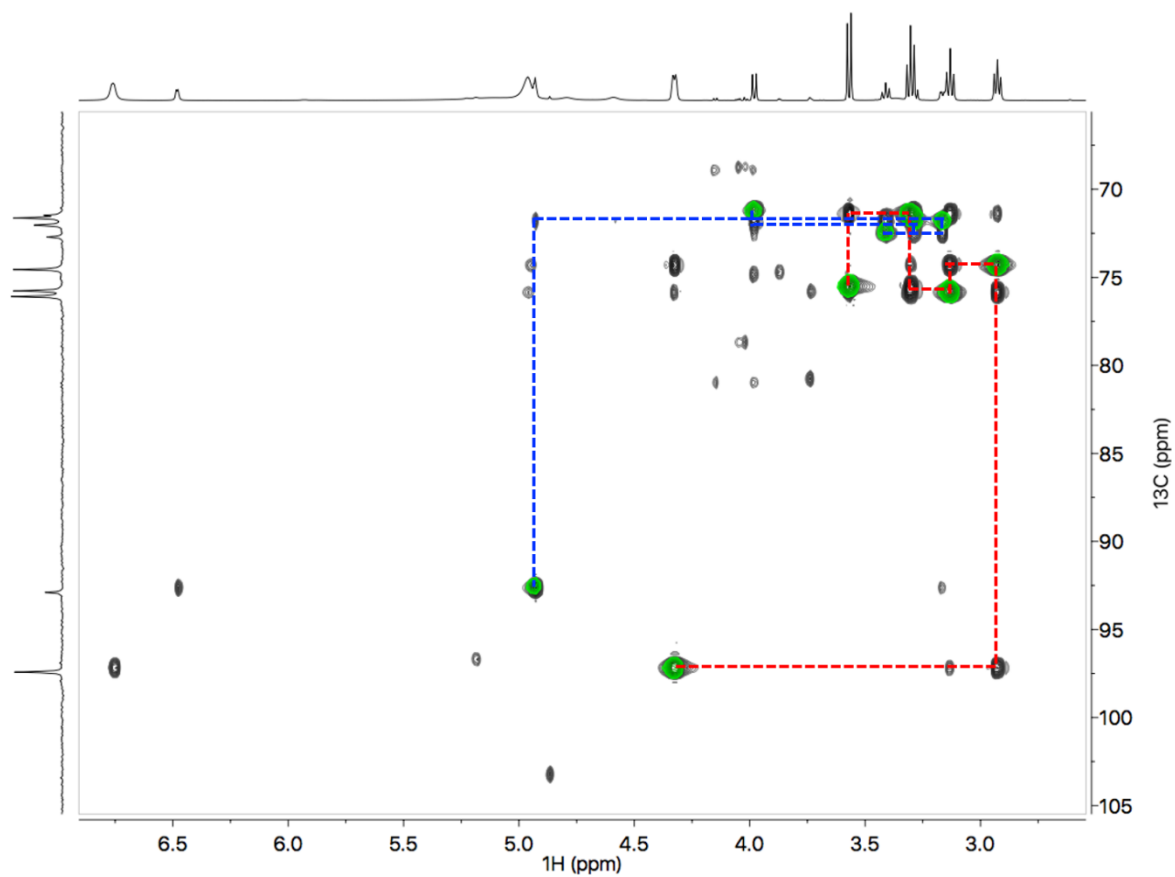


Figure S13 Glucuronic acid spectra at 65 °C in DMSO- d_6 (5 wt %): overlay of the 2D HSQC (1024 time-domain data size in f1, corresponding to 512 actual t_1 -increments) and HSQC-TOCSY (15ms) with CH1-CH5 correlations of α -glucuronic (red) and β -glucuronic (blue) acids. Overlay spectrum cross-peaks are blue/green for HSQC layer and grayscale for HSQC-TOCSY

3.13. Cellobiose NMR Assignment Supplementary

Table S4 Full peak assignment of α -cellobiose (Cb- α) referenced to [P₄₄₄₄][OAc]:DMSO-d₆ (20:80, ¹H: δ = 2.50 ppm, ¹³C: δ = 39.52 ppm) and D₂O at 30 °C (¹H: δ = 4.79 ppm, *italics*, Roslund et al. 2008)

Cb-NRE- α	¹ H, ppm	¹ H, ppm	¹³ C, ppm	¹³ C, ppm	Cb-RE- α	¹ H, ppm	¹ H, ppm	¹³ C, ppm	¹³ C, ppm
1	4.28(d) <i>J</i> = 6.7 Hz	4.50 <i>J</i> = 8.0 Hz	103.01	103.20	1	4.90 (d) <i>J</i> = 3.6 Hz	5.21 <i>J</i> = 3.8 Hz	91.97	92.46
2	2.99 (m)	3.31	73.28	73.82	2	3.14 (m)	3.57	72.59	71.87
3	3.25 (m)	3.50	76.05	76.16	3	3.61 (m)	3.81	71.36	71.98
4	3.14 (m)	3.41	69.52	70.12	4	3.25 (m)	3.63	80.68	79.43
5	3.08 (m)	3.48	77.05	76.63	5	3.61 (m)	3.94	69.42	70.75
6	3.61 (m)	3.91; 3.73	60.52	61.25	6	3.61 (m)	3.87; 3.85	60.70	60.60

Table S5 Full peak assignment of β -cellobiose (Cb- β) referenced to [P₄₄₄₄][OAc]:DMSO-d₆ (20:80, ¹H: δ = 2.50 ppm, ¹³C: δ = 39.52 ppm) and D₂O at 30 °C (¹H: δ = 4.79 ppm, *italics*, Roslund et al. 2008)

Cb-NRE- β	¹ H, ppm	¹ H, ppm	¹³ C, ppm	¹³ C, ppm	Cb-RE- β	¹ H, ppm	¹ H, ppm	¹³ C, ppm	¹³ C, ppm
1	4.26 (d) <i>J</i> = 7.8 Hz	4.50 <i>J</i> = 7.9 Hz	103.17	103.16	1	4.22 (d) <i>J</i> = 7.7 Hz	4.65 <i>J</i> = 8.0 Hz	97.57	96.39
2	2.99 (m)	3.30	73.34	73.81	2	3.08 (m)	3.27	73.84	74.54
3	3.25 (m)	3.50	76.07	76.16	3	3.25 (m)	3.61	74.54	74.94
4	3.14 (m)	3.41	69.49	70.11	4	3.25 (m)	3.64	80.82	79.30
5	3.08 (m)	3.48	77.09	76.63	5	3.14 (m)	3.59	74.59	75.43
6	3.61 (m)	3.90; 3.72	60.50	61.23	6	3.61 (m)	3.94; 3.80	60.73	60.73

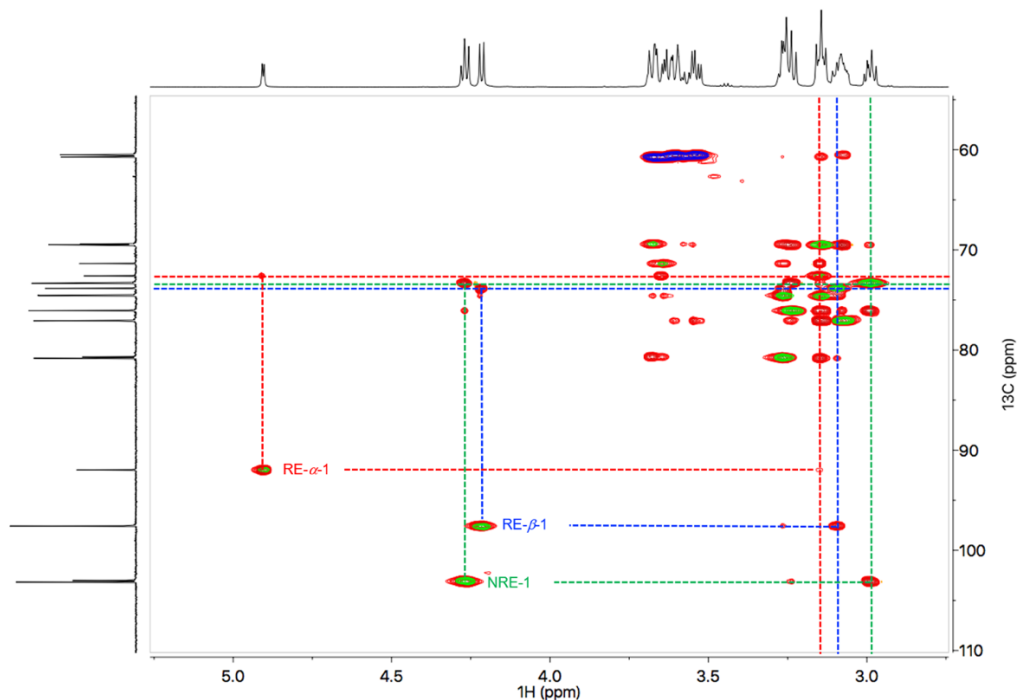


Figure S14 Cellobiose spectra at 65 °C in [P₄₄₄₄][OAc]:DMSO-d₆ (5 wt %): overlay of the multiplicity-edited 2D HSQC (2048 time-domain data size in f1, corresponding to 1024 actual t₁-increments) and HSQC-TOCSY (15ms) with CH1-CH2 correlations of cellobiose non-reducing end (green), α - and β -cellobiose reducing ends (red and blue respectively). Overlay spectrum cross-peaks are blue/green for HSQC layer and red for HSQC-TOCSY

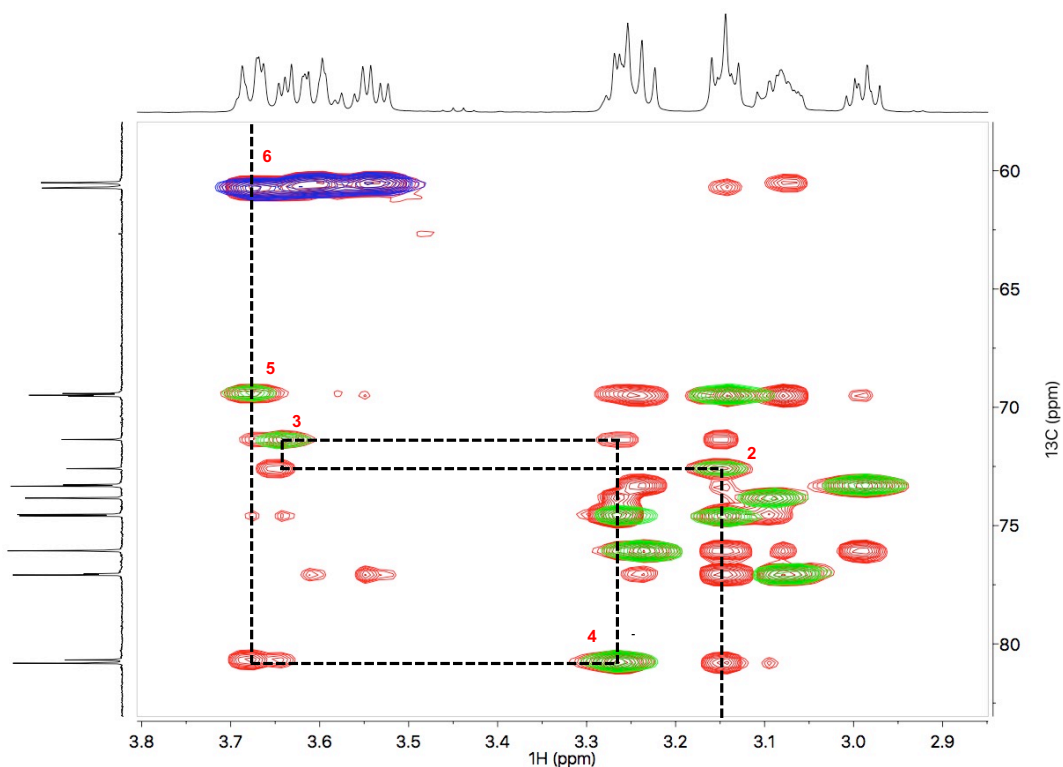


Figure S15 Cellobiose spectra at 65 °C in [P₄₄₄₄][OAc]:DMSO-d₆ (5 wt %): overlay of the multiplicity-edited 2D HSQC (2048 time-domain data size in f1, corresponding to 1024 actual t₁-increments) and HSQC-TOCSY (15ms) with CH₂-CH₆ correlations of α-cellobiose reducing end (red). Overlay spectrum cross-peaks are blue/green for HSQC layer and red for HSQC-TOCSY

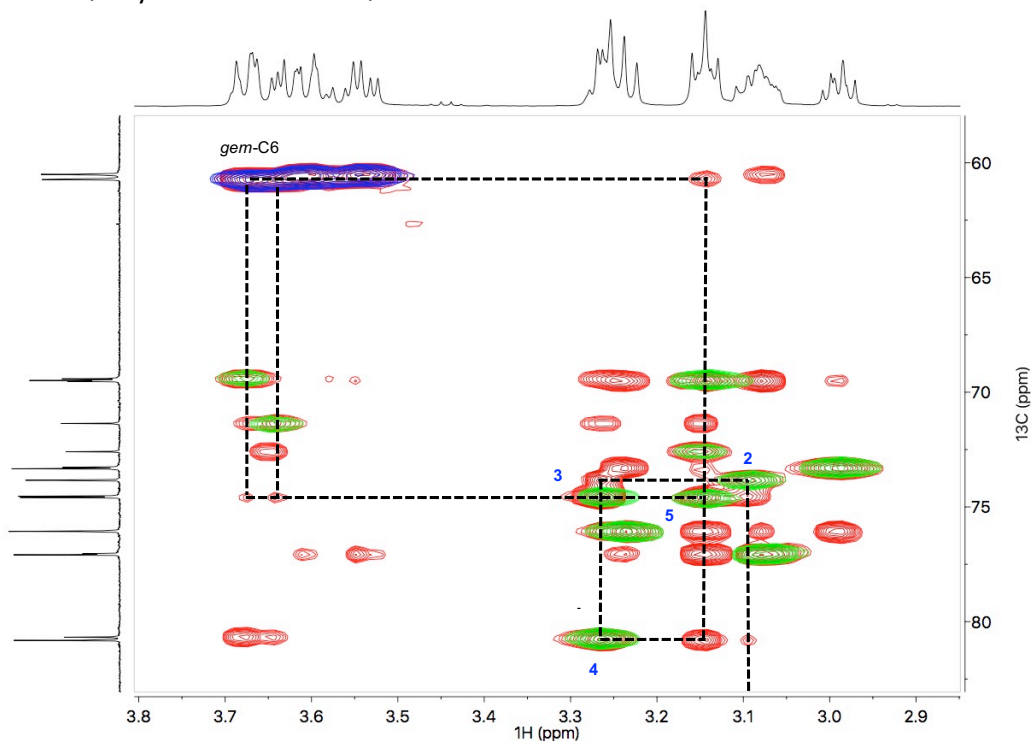


Figure S16 Cellobiose spectra at 65 °C in [P₄₄₄₄][OAc]:DMSO-d₆ (5 wt %): overlay of the multiplicity-edited 2D HSQC (2048 time-domain data size in f1, corresponding to 1024 actual t₁-increments) and HSQC-TOCSY (15ms) with CH₂-CH₆ correlations of β-cellobiose reducing end (blue). Overlay spectrum cross-peaks are blue/green for HSQC layer and red for HSQC-TOCSY

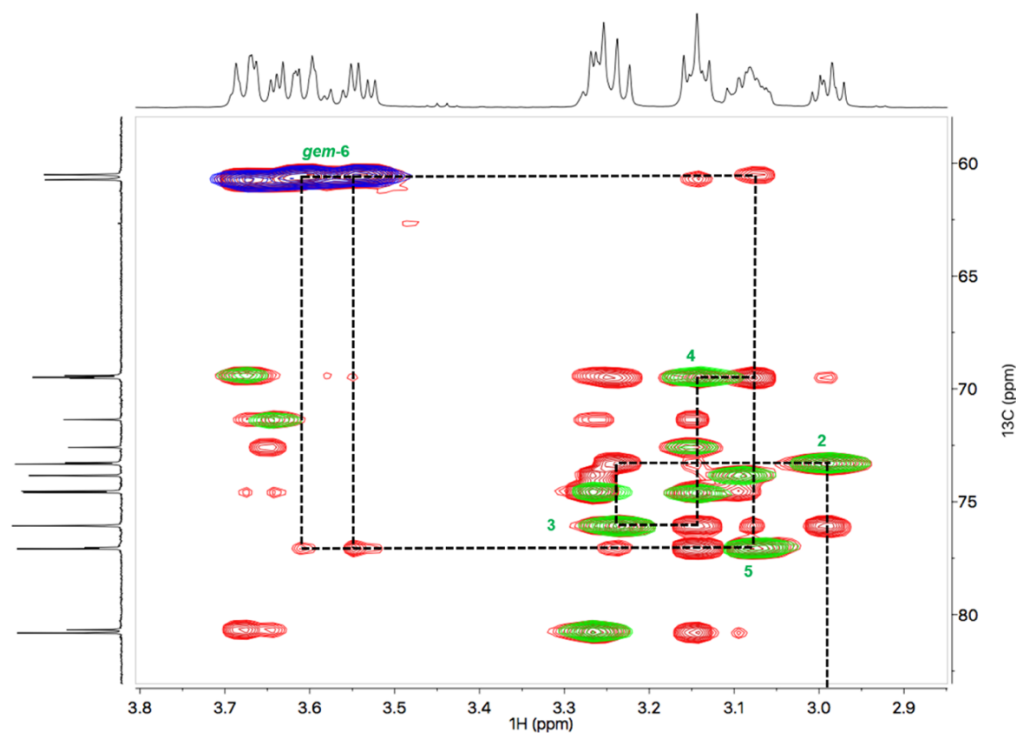


Figure S17 Cellobiose spectra at 65 °C in $[P_{4444}][OAc]:DMSO-d_6$ (5 wt %): overlay of the multiplicity-edited 2D HSQC (2048 time-domain data size in f1, corresponding to 1024 actual t_1 -increments) and HSQC-TOCSY (15ms) with CH2-CH6 correlations of cellobiose non-reducing end (green). Overlay spectrum cross-peaks are blue/green for HSQC layer and red for HSQC-TOCSY

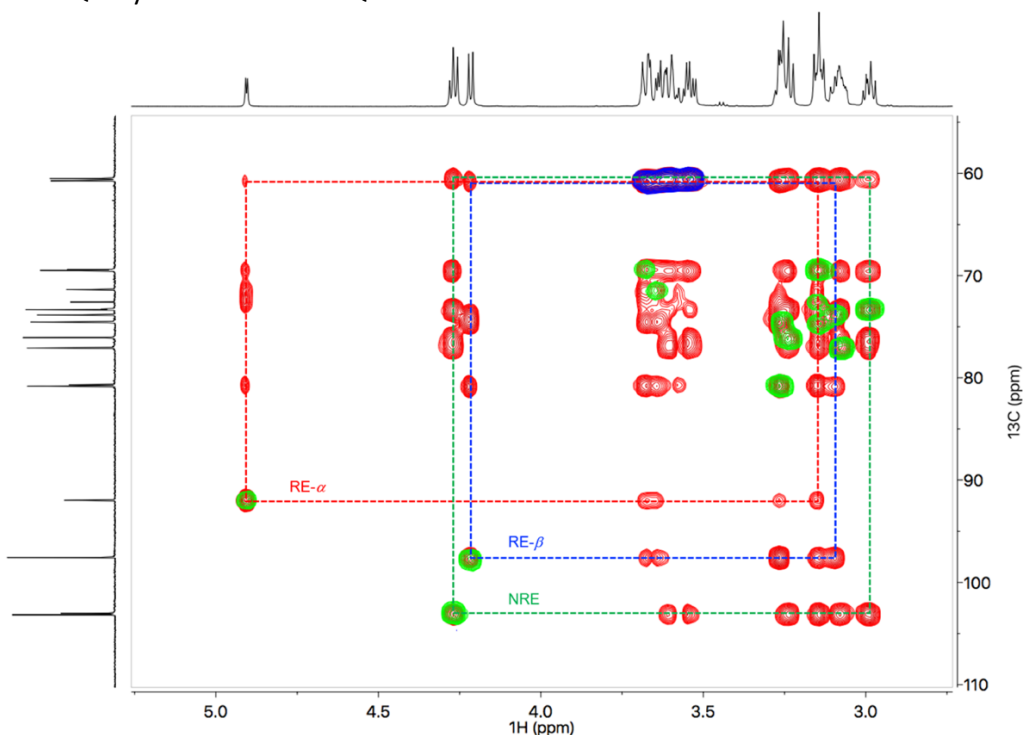


Figure S18 Cellobiose spectra at 65 °C in $[P_{4444}][OAc]:DMSO-d_6$ (5 wt %): overlay of the multiplicity-edited 2D HSQC (2048 time-domain data size in f1, corresponding to 1024 actual t_1 -increments) and HSQC-TOCSY (120ms) with CH1-CH6 correlations of cellobiose non-reducing end (green), α - and β -cellobiose reducing ends (red and blue respectively). Overlay spectrum cross-peaks are blue/green for HSQC layer and red for HSQC-TOCSY

3.14. Low-DP Cellulose NMR Assignment Supplementary

Table S6 Full peak assignment of LDP-CNC referenced to $[P_{4444}][OAc]:DMSO-d_6$ (20:80, 1H : $\delta = 2.50$ ppm, ^{13}C : $\delta = 39.52$ ppm)

Glc- NRE	1H , ppm	^{13}C , ppm	Glc- AGU	1H , ppm	^{13}C , ppm	Glc- RE- β	1H , ppm	^{13}C , ppm	Glc- RE- α	1H , ppm	^{13}C , ppm
1	4.30 (d) J = 7.8 Hz	102.76	1	4.40 (d) J = 7.4 Hz	102.38	1	4.21 (d) J = 7.7 Hz	97.62	1	4.90 (d) J = 3.4 Hz	91.99
2	3.06 (m)	73.17	2	3.06 (m)	72.97	2	3.06 (m)	73.81	2	3.06 (m)	72.65
3	3.33 (m)	76.04	3	3.33 (m)	74.39	3	3.33 (m)	74.52	3	3.63 (m)	69.48
4	3.06 (m)	69.60	4	3.33 (m)	78.40	4	3.33 (m)	80.49	4	3.33 (m)	80.28
5	3.06 (m)	77.23	5	3.33 (m)	75.19	5	3.06 (m)	74.66	5	3.63 (m)	71.40
6	3.63 (m)	60.62	6	3.63 (m)	60.03	6	3.63 (m)	60.27	6	3.63 (m)	60.35

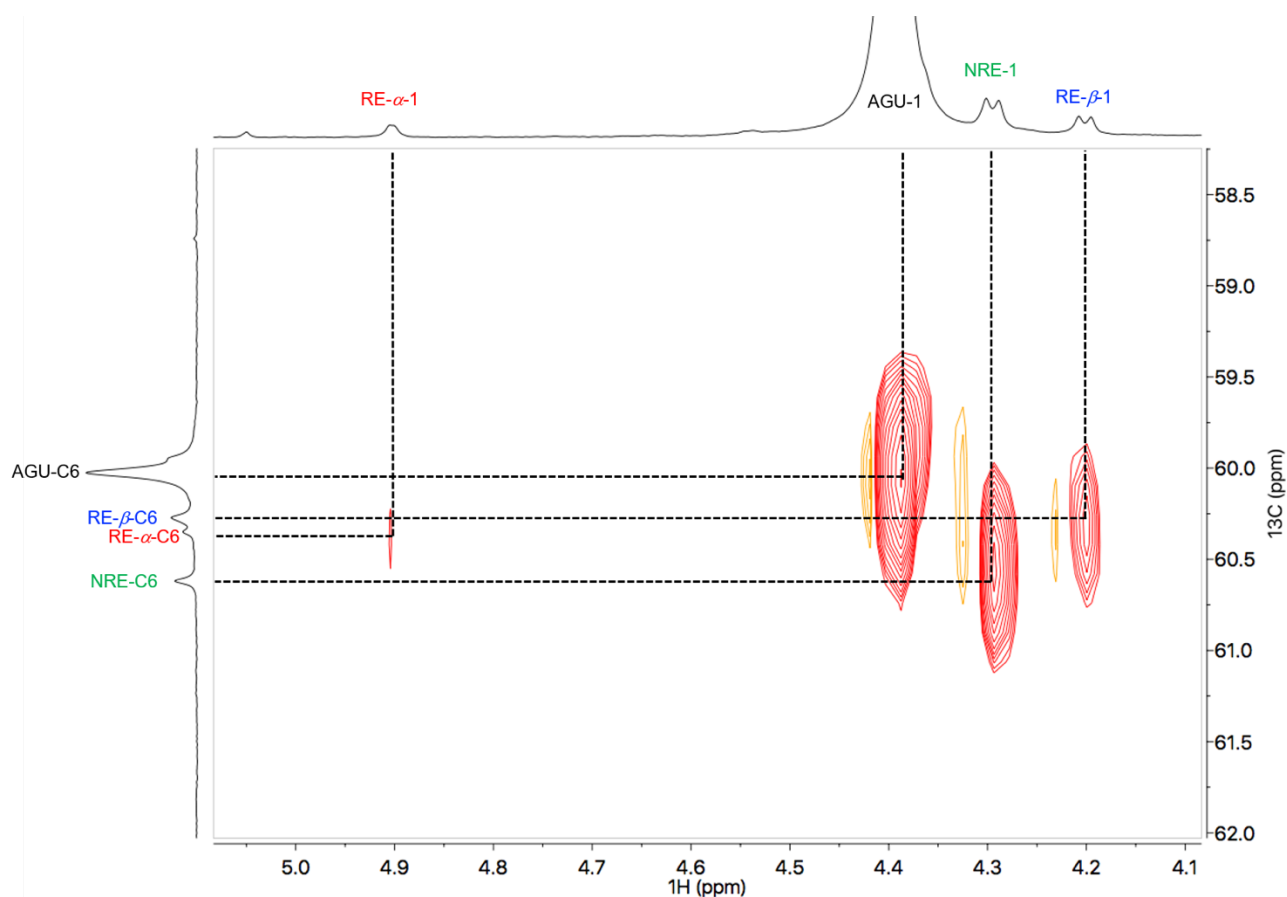


Figure S19 LDP-CNC spectra at 65 °C in $[P_{4444}][OAc]:DMSO-d_6$ (5 wt %): 2D HMBC (512 time-domain data size in f1, also corresponding here to 512 actual t_1 -increments) showing C1-CH6 correlations of non-reducing end (green), α - and β -reducing ends (red and blue respectively) and anhydrous glucose unit (black)

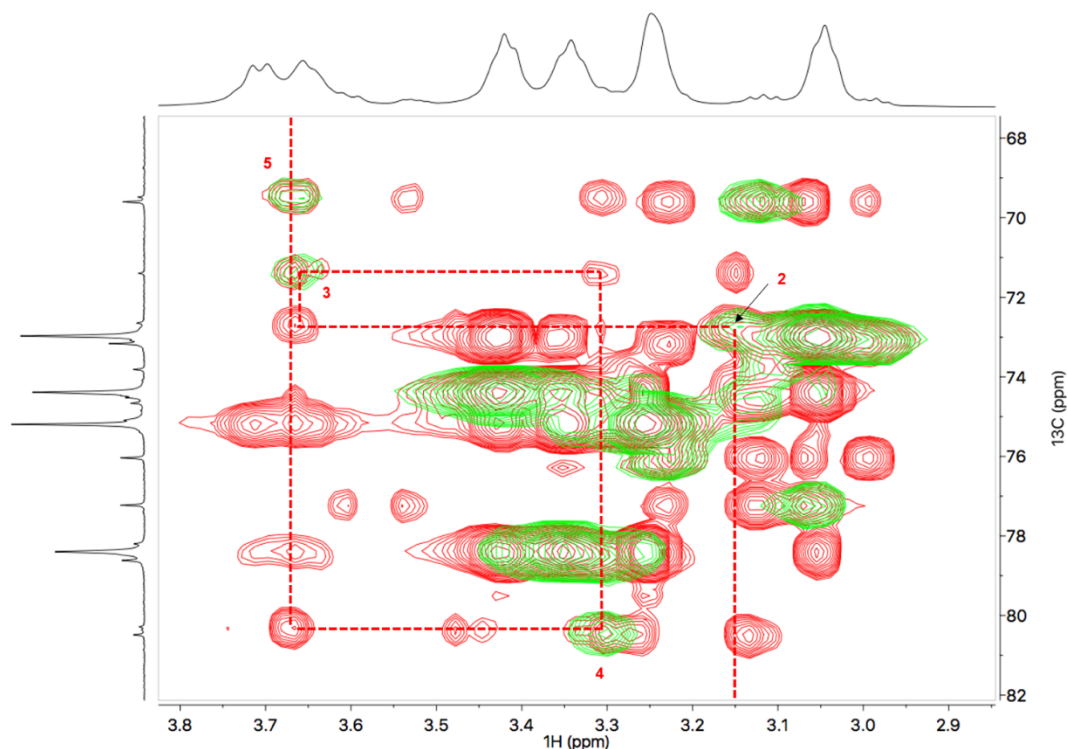


Figure S20 LDP-CNC spectra at 65 °C in $[P_{4444}][OAc]:DMSO-d_6$ (5 wt %): overlay of the multiplicity-edited 2D HSQC (512 time-domain data size in f1, corresponding to 256 actual t_1 -increments) and HSQC-TOCSY (25ms) with CH2-CH5 correlations of LDP-CNC α -reducing end (red). Overlay spectrum cross-peaks are blue/green for HSQC layer and red for HSQC-TOCSY

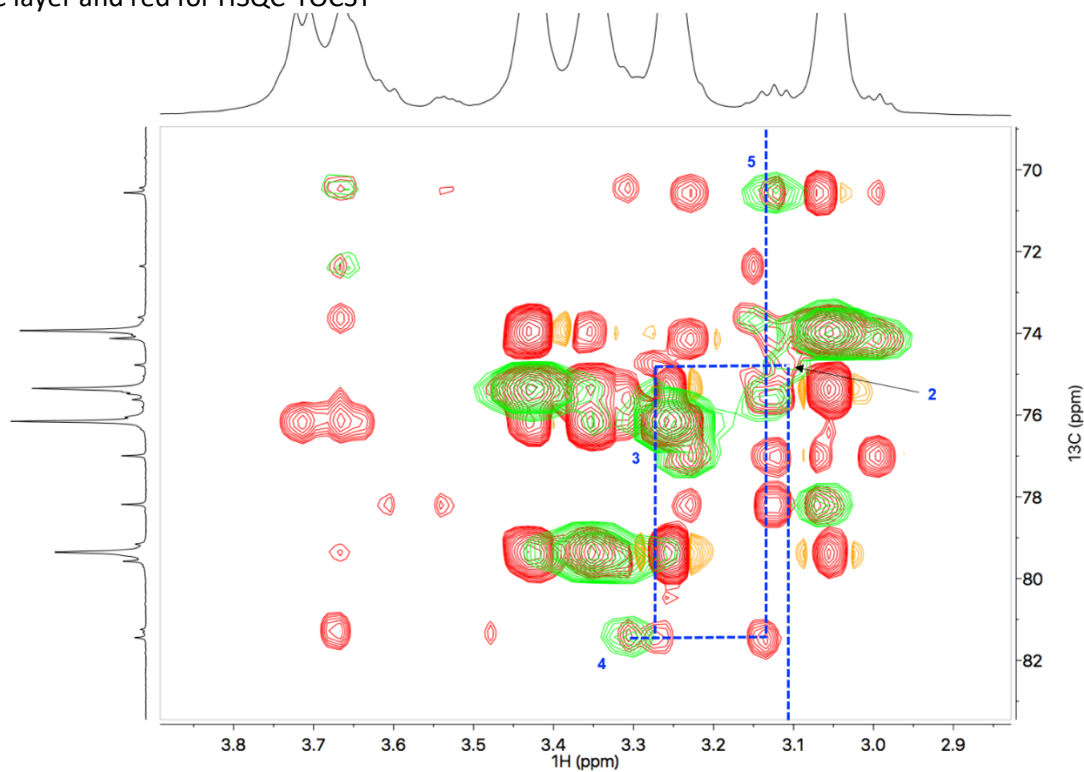


Figure S21 LDP-CNC spectra at 65 °C in $[P_{4444}][OAc]:DMSO-d_6$ (5 wt %): overlay of the multiplicity-edited 2D HSQC (512 time-domain data size in f1, corresponding to 256 actual t_1 -increments) and HSQC-TOCSY (25ms) with CH2-CH5 correlations of LDP-CNC β -reducing end (blue). Overlay spectrum cross-peaks are blue/green for HSQC layer and red for HSQC-TOCSY

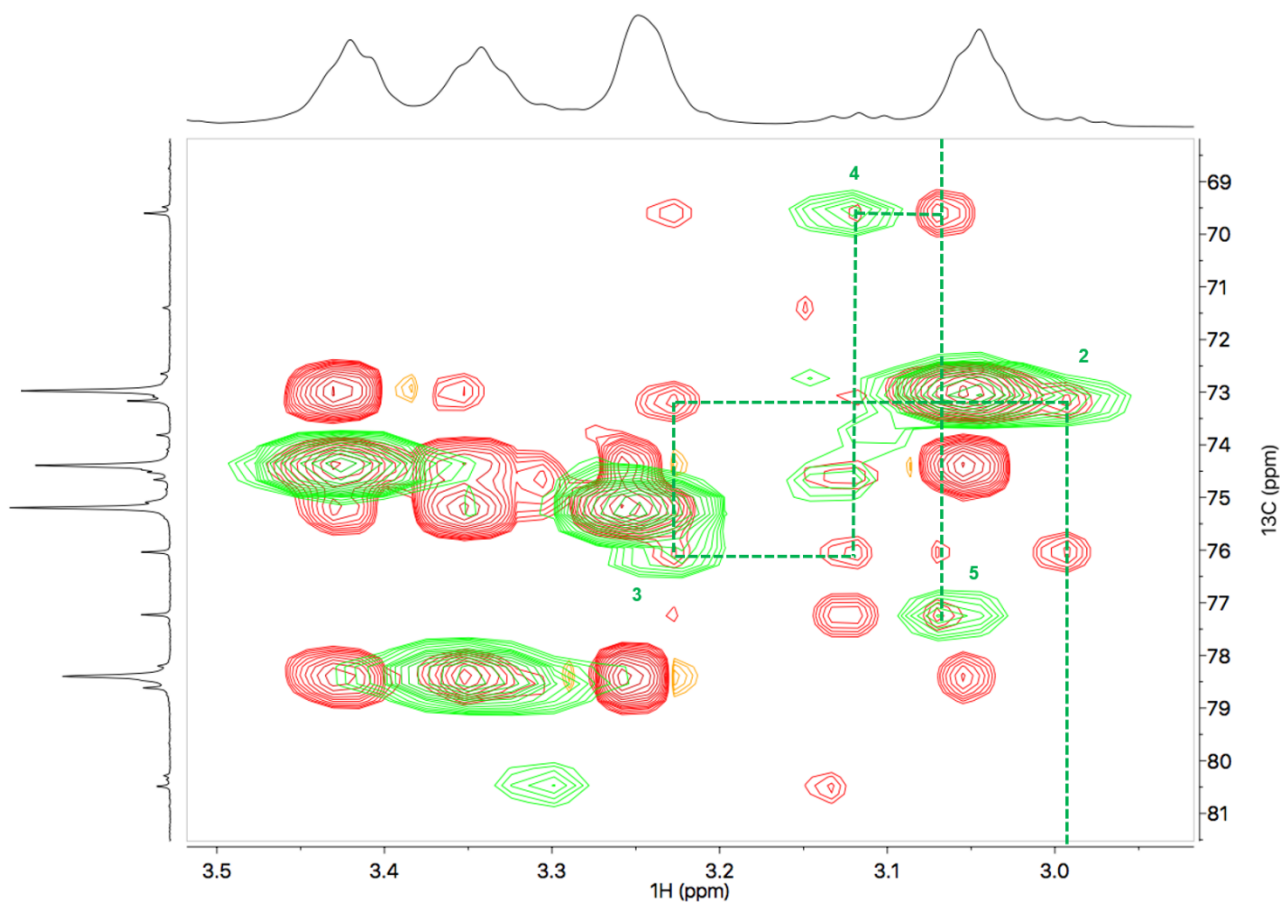


Figure S22 LDP-CNC spectra at 65 °C in $[P_{4444}][OAc]:DMSO-d_6$ (5 wt %): overlay of the multiplicity-edited 2D HSQC (512 time-domain data size in f1, corresponding to 256 actual t_1 -increments) and HSQC-TOCSY (25ms) with CH2-CH5 correlations of LDP-CNC non-reducing end (green). Overlay spectrum cross-peaks are blue/green for HSQC layer and red for HSQC-TOCSY

3.15. Nitroxyl-Radical Oxidized Low-DP Cellulose NMR Assignment Supplementary

Table S7. Full peak assignment of nitroxyl-radical oxidised low DP cellulose referenced to [P₄₄₄₄][OAc]:DMSO-d₆ (20:80, ¹H: δ = 2.50 ppm, ¹³C: δ = 39.52 ppm) and polyglucuronic acid in D₂O at 60 °C (¹H: δ = 4.79 ppm, *italics*, Tahiri and Vignon 2000)

Glc- NRE	¹ H, ppm	¹³ C, ppm	Glc- AGA	¹ H, ppm	¹ H, <i>ppm</i>	¹³ C, ppm	¹³ C, <i>ppm</i>	¹³ C, <i>ppm</i>	Glc- AGU	¹ H, ppm	¹³ C, ppm
1	4.10 (d) J = 7.7 Hz	102.85	1	4.19 (d) J = 5.9 Hz	4.43	104.26	103.55	1	4.39 (d) J = 7.3 Hz	102.41	
2	3.20 (m)	73.18	2	3.20 (m)	3.26	72.72	74.00	2	3.20 (m)	72.96	
3	3.20 (m)	76.16	3	3.20 (m)	3.51	76.16	75.50	3	3.20 (m)	74.46	
4	3.20 (m)	69.86	4	3.20 (m)	3.60	84.21	82.10	4	3.20 (m)	78.58	
5	3.20 (m)	77.11	5	3.20 (m)	3.76	73.96	76.60	5	3.20 (m)	75.17	
6	3.63 (m)	60.84	6	-		169.15	175.75	6	3.63 (m)	60.17	

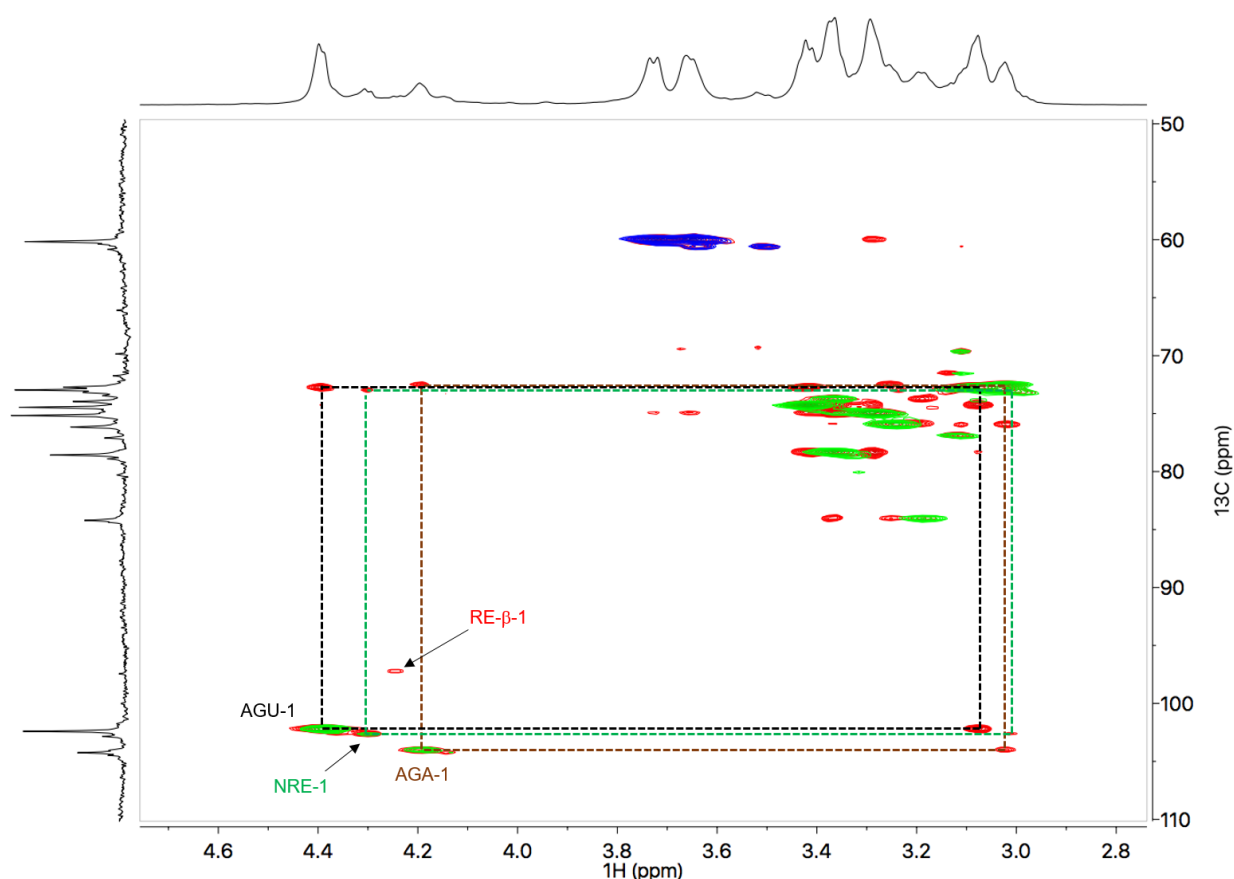


Figure S23 Nitroxyl-radical oxidized LDP-CNC spectra at 65 °C in [P₄₄₄₄][OAc]:DMSO-d₆ (5 wt %): overlay of the multiplicity-edited 2D HSQC (1024 time-domain data size in f1, corresponding to 512 actual t₁-increments) and HSQC-TOCSY (15ms) with CH1-CH2 correlations of nitroxyl-radical oxidized LDP-CNC non-reducing end (**green**), anhydroglucuronic acid (**brown**) and internal (middle chain) non-oxidized anhydrous glucose unit resonances (**black**). Overlay spectrum cross-peaks are blue/green for HSQC layer and red for HSQC-TOCSY

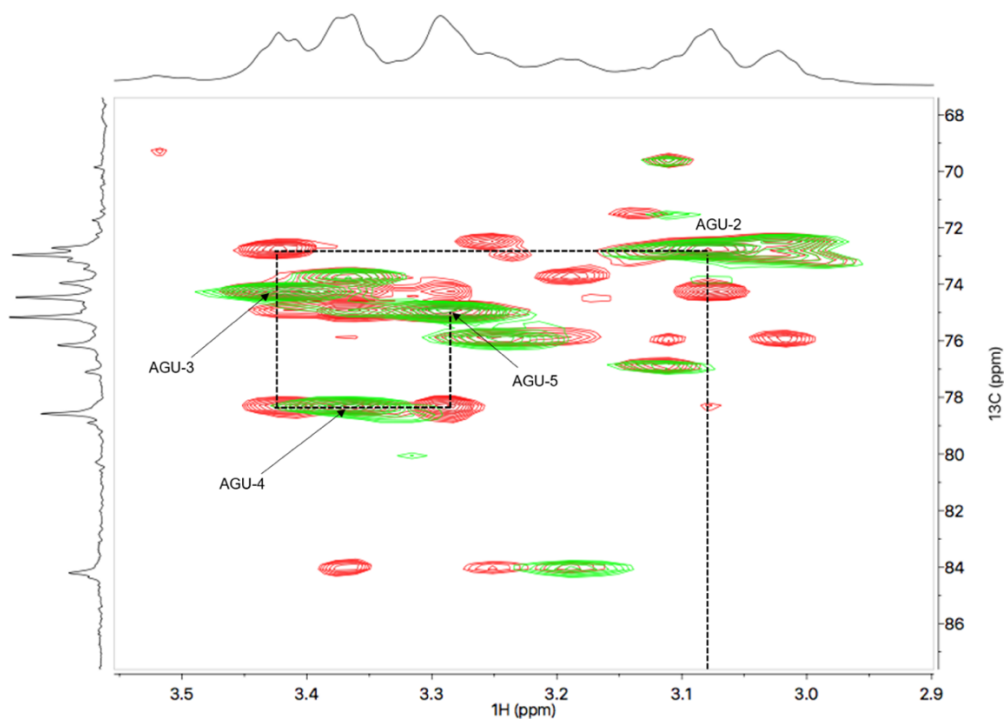


Figure S24 Nitroxyl-radical oxidized LDP-CNC spectra at 65 °C in $[\text{P}_{4444}][\text{OAc}]:\text{DMSO-d}_6$ (5 wt %): overlay of the multiplicity-edited 2D HSQC (1024 time-domain data size in f1, corresponding to 512 actual t_1 -increments) and HSQC-TOCSY (15ms) with CH2-CH5 correlations of internal (middle chain) non-oxidized anhydrous glucose unit resonances (black). Overlay spectrum cross-peaks are blue/green for HSQC layer and red for HSQC-TOCSY

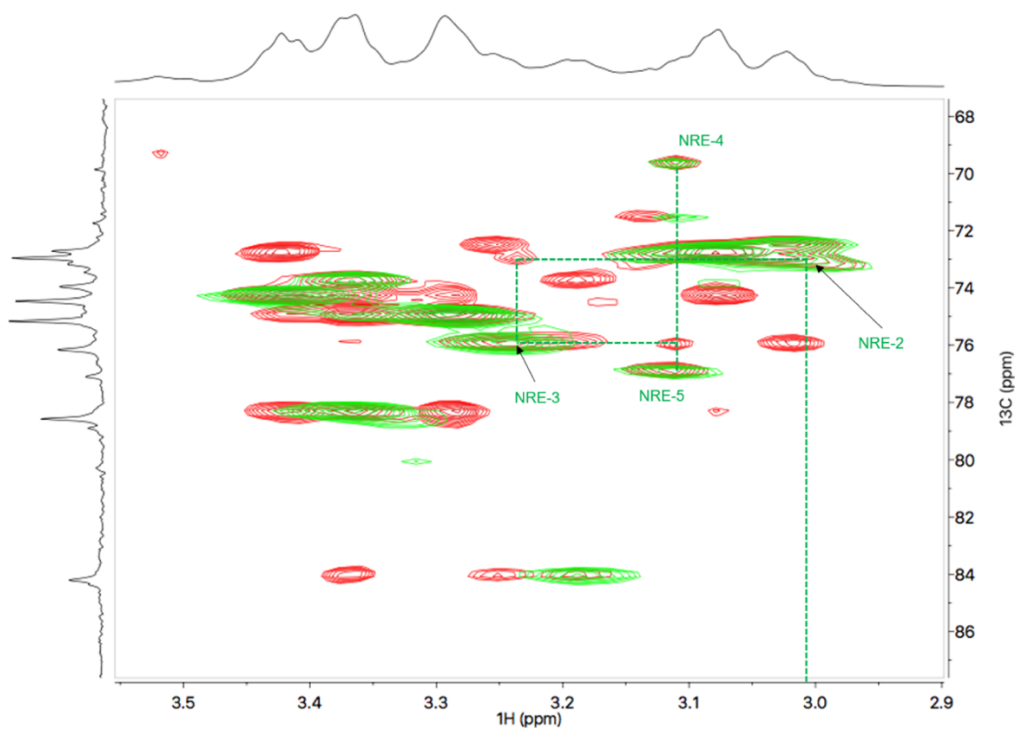


Figure S25 Nitroxyl-radical oxidized LDP-CNC spectra at 65 °C in $[\text{P}_{4444}][\text{OAc}]:\text{DMSO-d}_6$ (5 wt %): overlay of the multiplicity-edited 2D HSQC (1024 time-domain data size in f1, corresponding to 512 actual t_1 -increments) and HSQC-TOCSY (15ms) with CH2-CH5 correlations of non-reducing end resonances (green). Overlay spectrum cross-peaks are blue/green for HSQC layer and red for HSQC-TOCSY

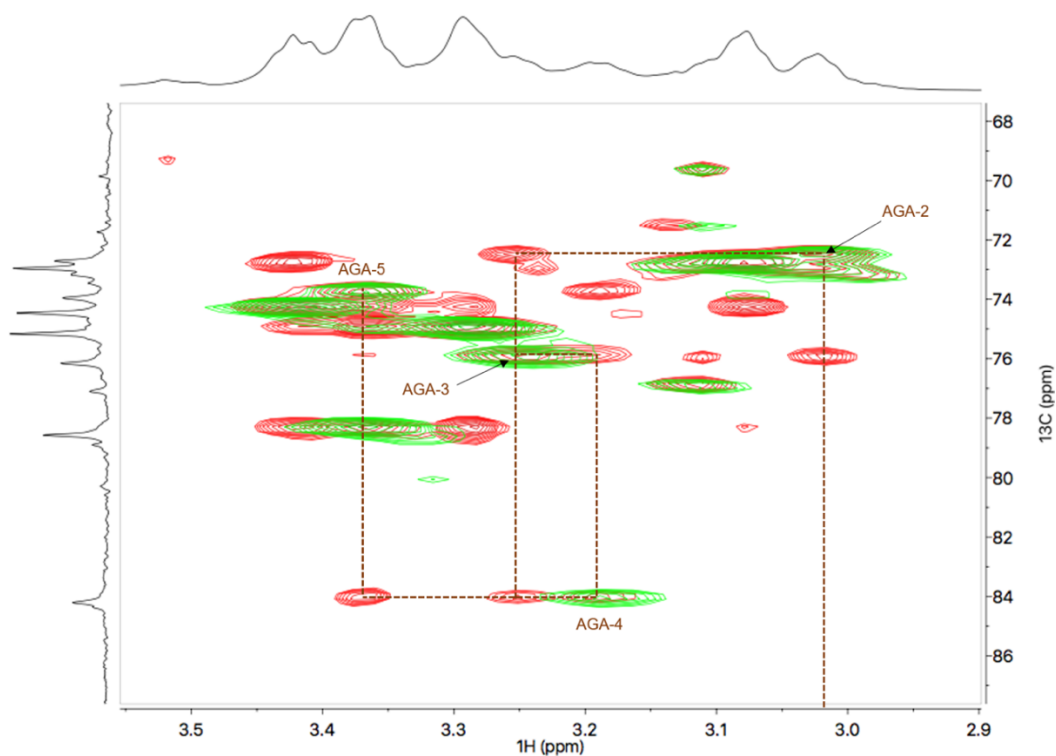


Figure S26 Nitroxyl-radical oxidized LDP-CNC spectra at 65 °C in [P₄₄₄₄][OAc]:DMSO-d₆ (5 wt %): overlay of the multiplicity-edited 2D HSQC (1024 time-domain data size in f1, corresponding to 512 actual t₁-increments) and HSQC-TOCSY (15ms) with CH₂-CH₅ correlations of internal anhydroglucuronic acid (**brown**). Overlay spectrum cross-peaks are blue/green for HSQC layer and red for HSQC-TOCSY

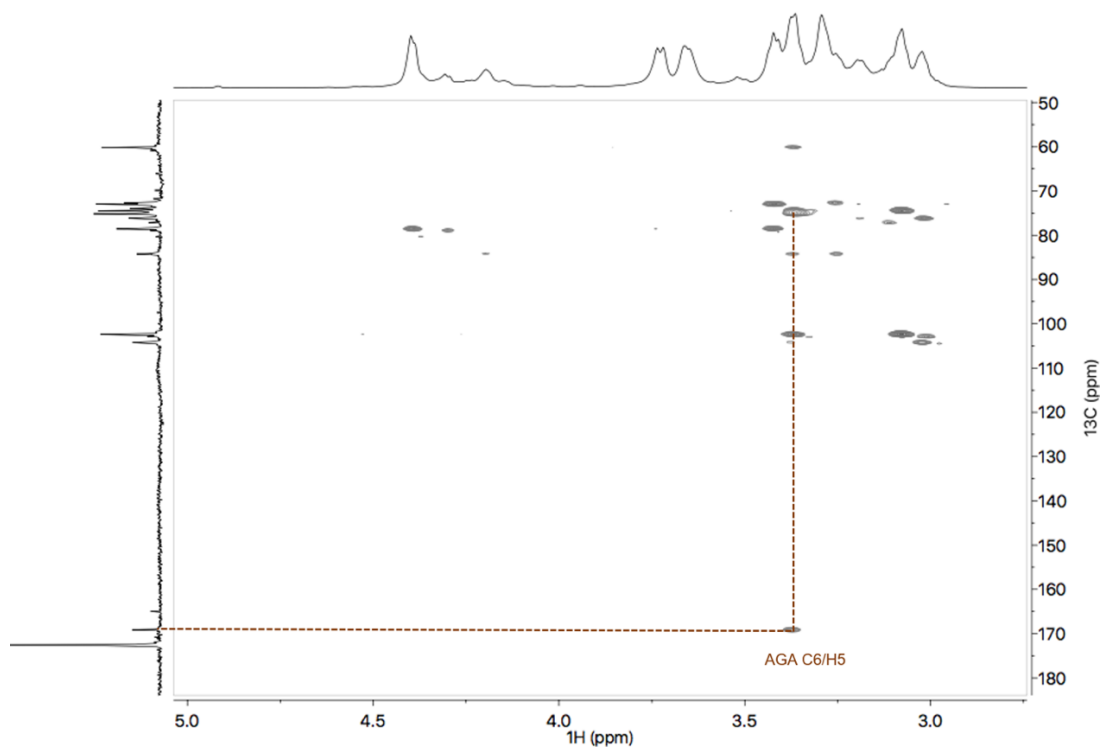


Figure S27 Nitroxyl-radical oxidized LDP-CNC spectra at 65 °C in [P₄₄₄₄][OAc]:DMSO-d₆ (5 wt %): 2D HMBC (512 time-domain data size in f1, also corresponding here to 512 actual t₁-increments) with C₆-CH₅ correlations of internal anhydroglucuronic acid (**brown**)

3.16. Cellobionic Acid NMR Assignment Supplementary

Table S8 Full peak assignment of cellobionic acid (acid form) referenced to [P₄₄₄₄][OAc]:DMSO-d₆ (20:80, ¹H: δ = 2.50 ppm, ¹³C: δ = 39.52 ppm) to D₂O at 65 °C (¹H: δ = 4.79 ppm, *italics*, Tomar et al. 2016)

Cb-NRE	¹ H, ppm	¹ H, ppm	¹³ C, ppm	¹³ C, ppm	Cb-Oxid-Acid	¹ H, ppm	¹ H, ppm	¹³ C, ppm	¹³ C, ppm
1	4.19 (d) J = 7.7 Hz	4.5	104.05	<i>103.0</i>	1	-		n/a	<i>178.3</i>
2	2.99 (m)	3.8	73.69	<i>73.4</i>	2	3.55 (m)	4.1	69.53	72.5
3	3.18 (t) J = 8.5 Hz	3.5	76.33	<i>75.5</i>	3	3.95 (m)	4.0	71.35	71.4
4	2.99 (m)	3.3	70.06	<i>69.5</i>	4	3.55 (m)	3.9	82.36	81.6
5	2.99 (m)	3.4	77.08	<i>76.0</i>	5	3.74 (td) J = 6.2; 3.4 Hz	3.9	72.01	71.7
6	3.55 (m)	3.8	61.16	<i>60.6</i>	6	3.55 (m)	3.7; 3.6	62.74	61.9

Table S9 Full peak assignment of cellobionic acid (lactone form) referenced to [P₄₄₄₄][OAc]:DMSO-d₆ (20:80, ¹H: δ = 2.50 ppm, ¹³C: δ = 39.52 ppm)

Cb-NRE	¹ H, ppm	¹³ C, ppm	Cb-Oxid-Lact	¹ H, ppm	¹³ C, ppm
1	4.34 (m)	102.44	1	-	n/a
2	2.99 (m)	72.97	2	3.95 (m)	70.73
3	3.21 (t) J = 8.3 Hz	76.17	3	3.82 (m)	72.97
4	2.99 (m)	69.87	4	3.82 (m)	76.99
5	2.99 (m)	77.08	5	4.34 (m)	79.38
6	3.55 (m)	60.70	6	3.55 (m)	59.94

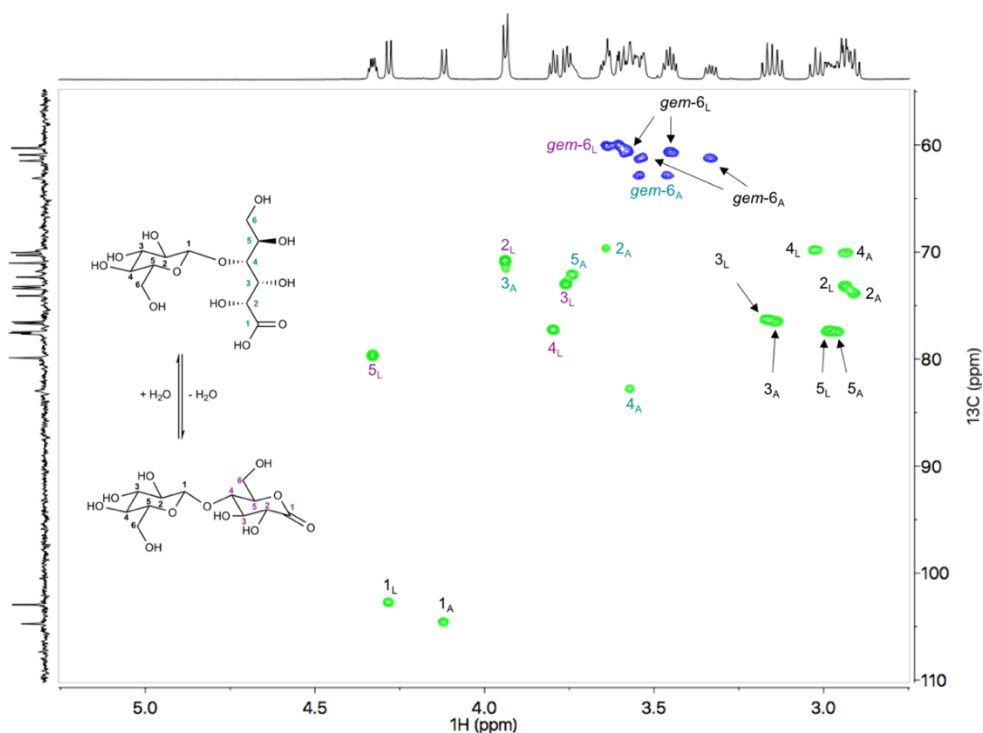


Figure S28 Cellobionic acid spectra at 27 °C in $[P_{4444}][OAc]:DMSO-d_6$ (5 wt %): multiplicity-edited 2D HSQC (512 time-domain data size in f1, corresponding to 256 actual t_1 -increments). Glucose unit resonances (black), open-chain acid unit (turquoise) and lactone unit (purple). 'A' and 'L' subscripts refer to 'acid' and 'lactone' forms

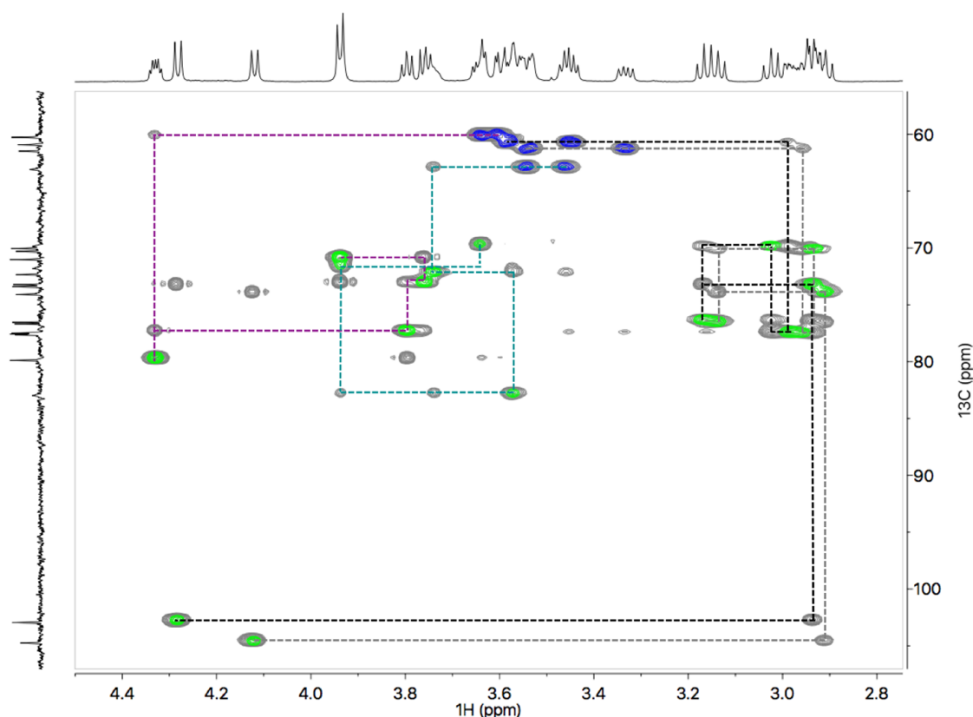


Figure S29 Cellobionic acid spectra at 27 °C in $[P_{4444}][OAc]:DMSO-d_6$ (5 wt %): overlay of the multiplicity-edited 2D HSQC (512 time-domain data size in f1, corresponding to 256 actual t_1 -increments) and HSQC-TOCSY (15ms). Glucose unit resonances (black for lactonic glucose and grey for acidic glucose), open-chain acid unit (turquoise) and lactone unit (purple). Overlay spectrum cross-peaks are blue/green for HSQC layer and grayscale for HSQC-TOCSY

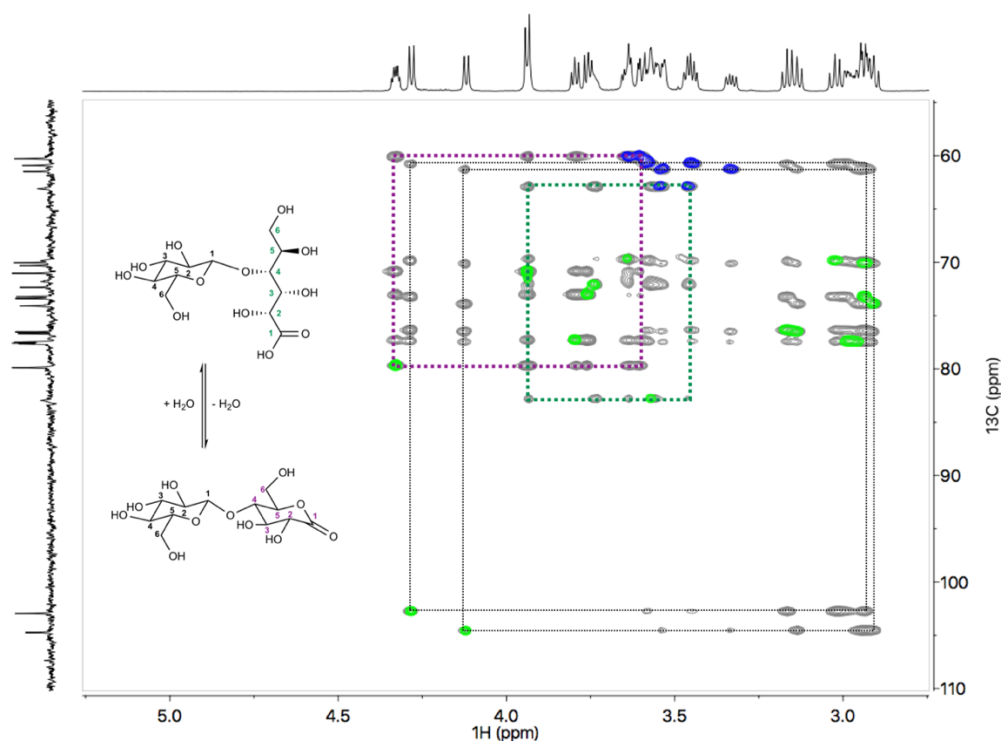


Figure S30 Cellobionic acid spectra at 27 °C in $[P_{4444}][OAc]:DMSO-d_6$ (5 wt): overlay of the multiplicity-edited 2D HSQC (512 time-domain data size in f_1 , corresponding to 256 actual t_1 -increments) and HSQC-TOCSY (120ms). Glucose unit resonances (black for lactonic glucose and grey for acidic glucose), open-chain acid unit (turquoise) and lactone unit (purple). Overlay spectrum cross-peaks are blue/green for HSQC layer and grayscale for HSQC-TOCSY

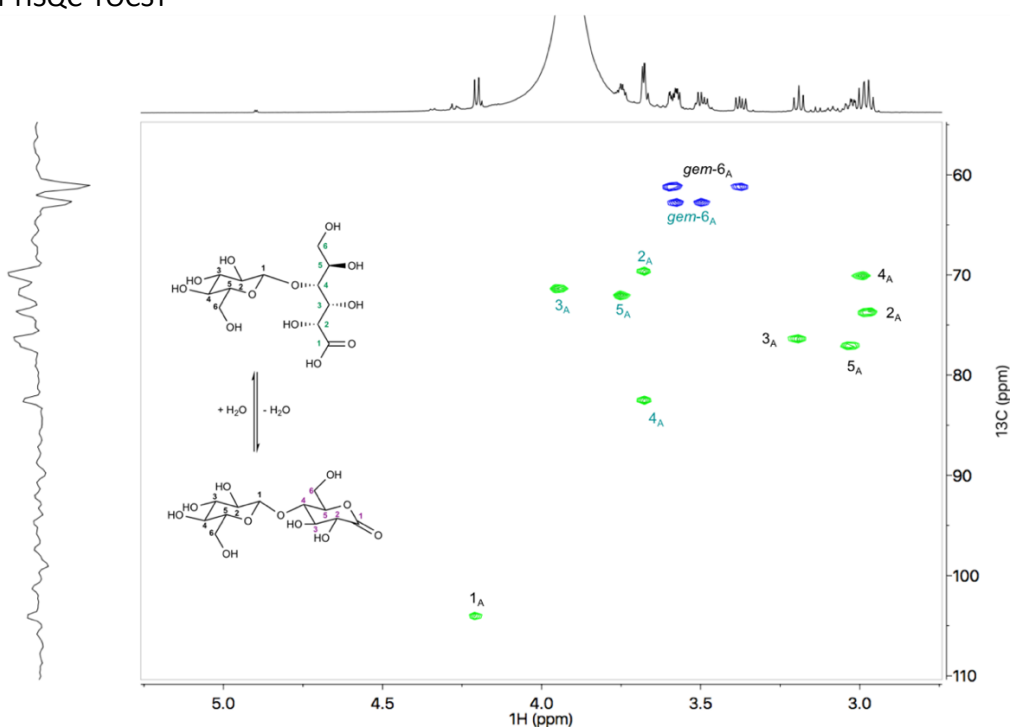


Figure S31 Cellobionic acid spectra at 65 °C in $[P_{4444}][OAc]:DMSO-d_6$ (5 wt) with 1 drop of water added to the NMR tube: multiplicity-edited 2D HSQC (512 time-domain data size in f_1 , corresponding to 256 actual t_1 -increments). Glucose unit resonances (black) and open-chain acid unit (turquoise) indicate presence of opened acid form only

3.17. Reducing End Oxidation to Carboxylates NMR Assignment Supplementary

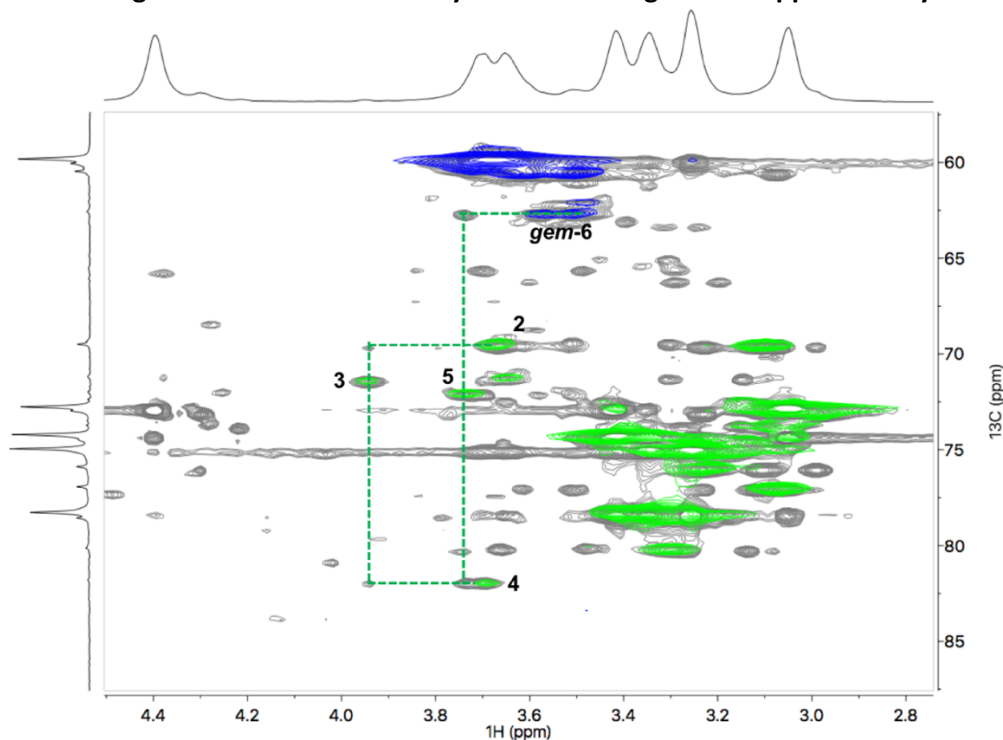


Figure S32 Reducing end (NaClO₂) oxidized low-DP cellulose spectra at 65 °C in [P₄₄₄₄][OAc]:DMSO-d₆ (5 wt): overlay of the multiplicity-edited 2D HSQC (1024 time-domain data size in f1, corresponding to 512 actual t₁-increments) and HSQC-TOCSY (15ms). 'Reducing end' gluconate form signals are marked. Overlay spectrum cross-peaks are blue/green for HSQC layer and grayscale for HSQC-TOCSY

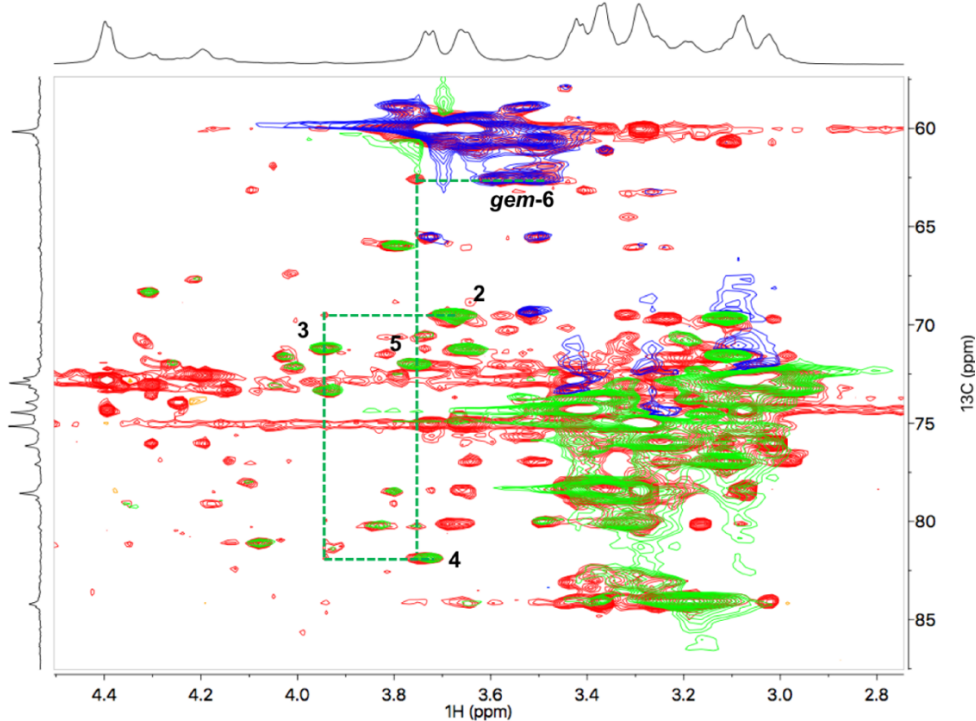


Figure S33 Reducing end (TEMPO) oxidized LDP-CNC spectra at 65 °C in [P₄₄₄₄][OAc]:DMSO-d₆ (5 wt): overlay of the multiplicity-edited 2D HSQC (1024 time-domain data size in f1, corresponding to 512 actual t₁-increments) and HSQC-TOCSY (15ms). 'Reducing end' gluconate form signals are marked. Overlay spectrum cross-peaks are blue/green for HSQC layer and red for HSQC-TOCSY

3.18. Periodate-Oxidized Cellulose NMR Supplementary

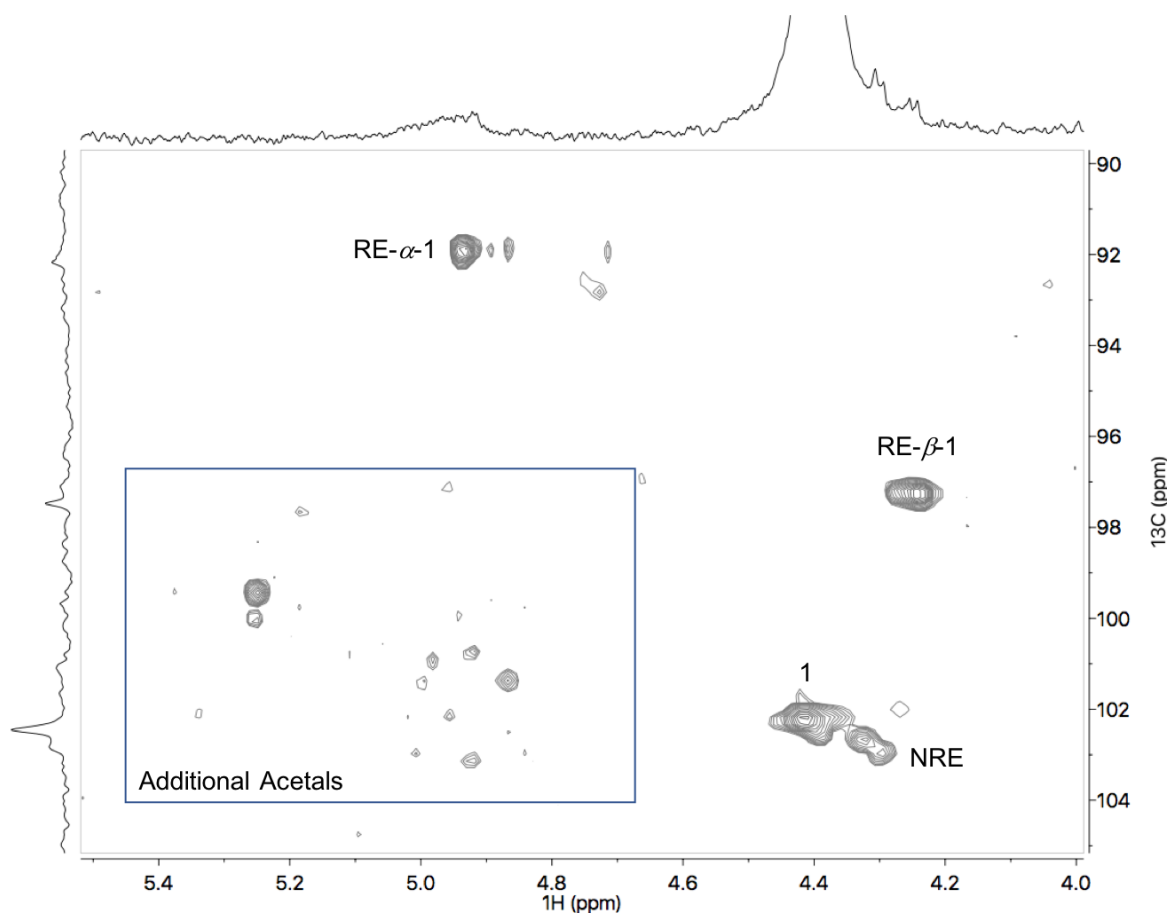


Figure S34 (Hemi)acetal region for the NaIO_4 -CNC spectra at 65 °C in $[\text{P}_{4444}][\text{OAc}]:\text{DMSO-d}_6$ (5 wt): 2D HSQC (1024 time-domain data size in f1, corresponding to 512 actual t_1 -increments)

3.19. Low-DP Cellulose Structural Data

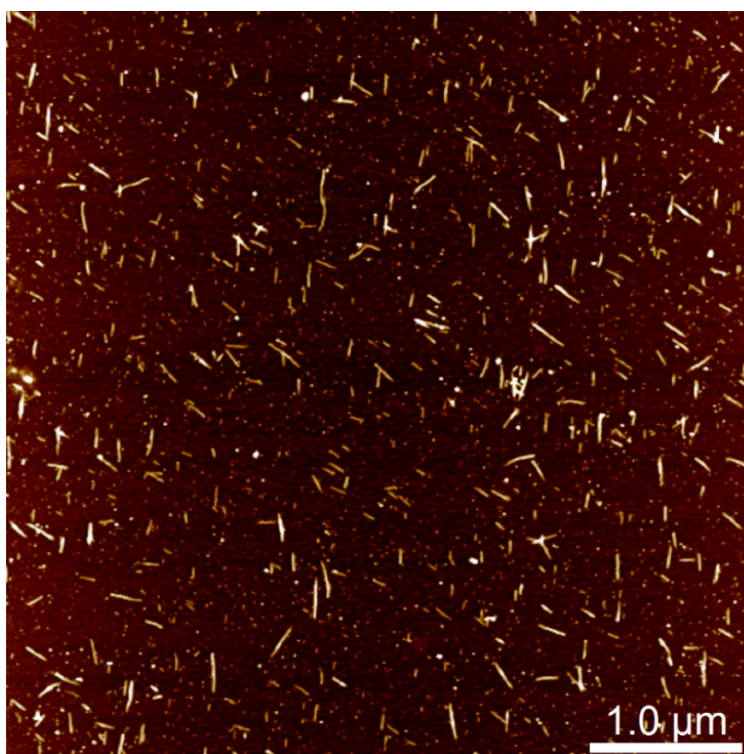


Figure S35 Atomic force microscopy (AFM) image of LDP-CNCs

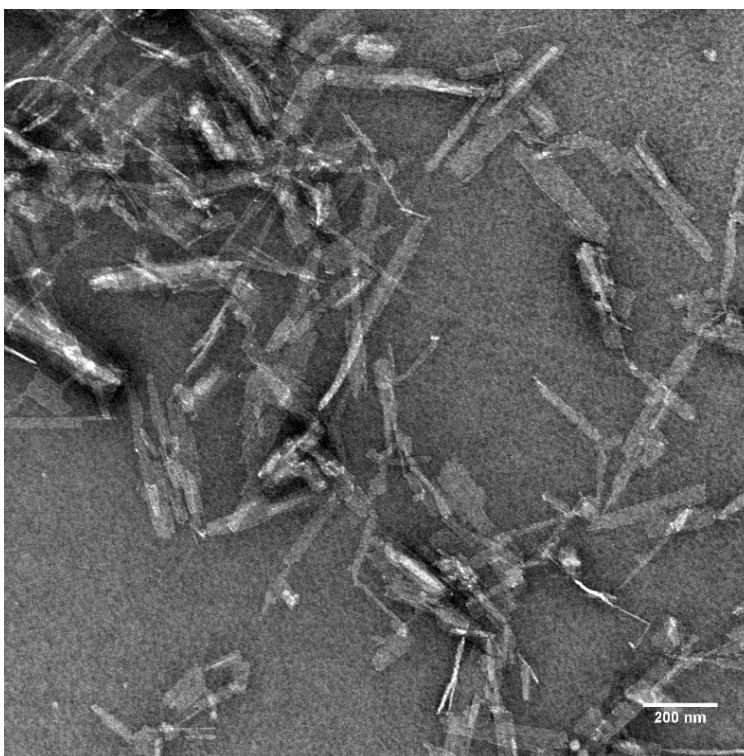


Figure S36 Transmission electron microscopy (TEM) image of LDP-CNCs

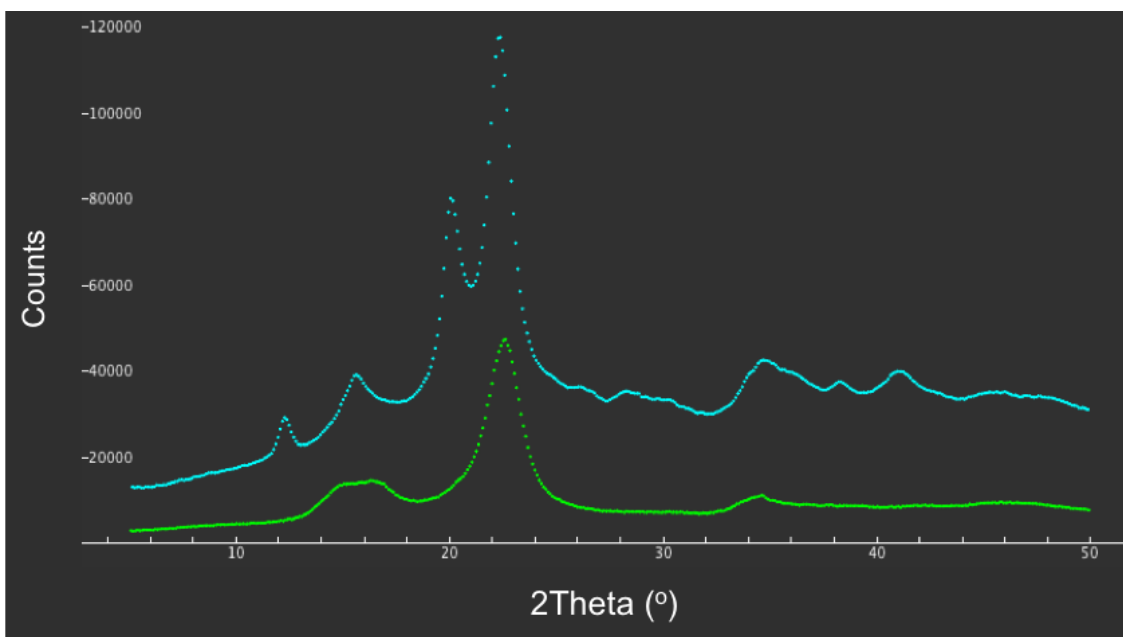


Figure S37 WAXS diffractograms: (a) LDP-CNCs (turquoise); (b) microcrystalline cellulose (green)

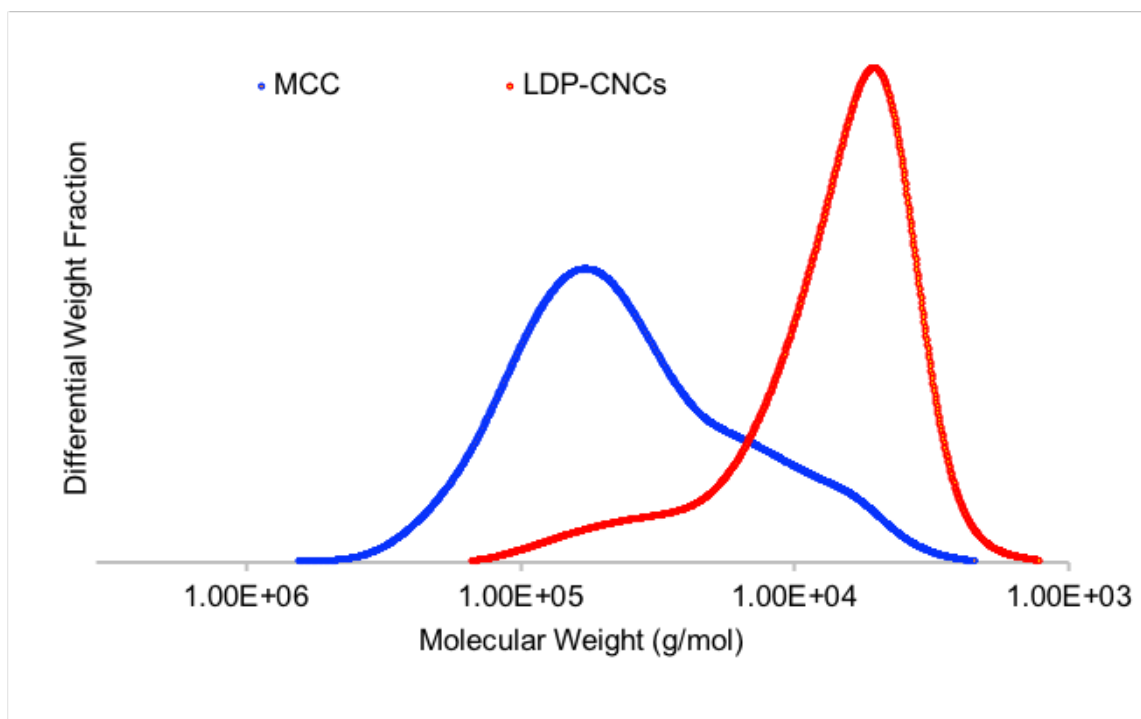


Figure S38 Molecular weight distribution for: (a) LDP-CNCs (red); (b) microcrystalline cellulose (blue)

References

- Agrawal PK (1992) NMR Spectroscopy in the structural elucidation of oligosaccharides and glycosides. *Phytochemistry* 31: 3307-3330. DOI: 10.1016/0031-9422(92)83678-R
- Bax A, Summers MF (1986) Proton and carbon-13 assignments from sensitivity-enhanced detection of heteronuclear multiple-bond connectivity by 2D multiple quantum NMR. *J. Am. Chem. Soc.* 108: 2093-2094. doi: 10.1021/ja00268a061
- Buffiere J, Ahvenainen P, Borrega M, Svedström K, Sixta H (2016) Supercritical Water Hydrolysis: A Green Pathway for Producing Low-Molecular-Weight Cellulose. *Green Chem.* 18: 6516–6525. DOI: 10.1039/C6GC02544G
- Fujisawa S, Isogai T, Isogai A (2010) Temperature and pH stability of cellouronic acid. *Cellulose* 17:607–615. doi: 10.1007/s10570-010-9407-9
- Hirota M, Tamura N, Saito T, Isogai A (2009) Oxidation of Regenerated Cellulose with NaClO₂ Catalyzed by TEMPO and NaClO under Acid-Neutral Conditions. *Carbohydr. Polym.* 78: 330–335. DOI: 10.1016/j.carbpol.2009.04.012
- Kay LE, Keifer P, Saarinen T (1992) Pure Absorption Gradient Enhanced Heteronuclear Single Quantum Correlation Spectroscopy with Improved Sensitivity. *J. Am. Chem. Soc.* 114: 10663-10665. DOI: 10.1021/ja00052a088
- King AWT, Mäkelä V, Kedzior SA, Laaksonen T, Partl GJ, Heikkinen S, Koskela H, Heikkinen HA, Holding AJ, Cranston ED, Kilpeläinen I (2018) Liquid-state NMR analysis of nanocelluloses. *Biomacromolecules* 19: 2708–2720. DOI: 10.1021/acs.biomac.8b00295
- Nypelö T, Amer H, Konnerth J, Potthast A, Rosenau T (2018) Self-Standing Nanocellulose Janus-Type Films with Aldehyde and Carboxyl Functionalities. *Biomacromolecules* 19: 973–979. DOI: 10.1021/acs.biomac.7b01751
- Palmer III AG, Cavanagh J, Wright PE, Rance M (1991) Sensitivity improvement in proton-detected two-dimensional heteronuclear correlation NMR spectroscopy. *J. Magn. Reson.* 93: 151-170. DOI: 10.1016/0022-2364(91)90036-S
- Roslund M, Tähtinen P, Niemitz M, Sjöholm R (2008) Complete assignments of the ¹H and ¹³C chemical shifts and J_{H,H} coupling constants in NMR spectra of D-glucopyranose and all D-glucopyranosyl-D-glucopyranosides. *Carbohydr. Res.* 343: 101-112. DOI: 10.1016/j.carres.2007.10.008
- Schleucher J, Schwendinger M, Sattler M, Schmidt P, Schedletzky O, Glaser SJ, Sorensen OW, Griesinger C (1994) A general enhancement scheme in heteronuclear multidimensional NMR employing pulsed field gradients. *J. Biomol. NMR* 4: 301-306. DOI: 10.1007/BF00175254
- Tolonen LK, Penttilä PA, Serimaa R, Kruse A, Sixta H (2013) The Swelling and Dissolution of Cellulose Crystallites in Subcritical and Supercritical Water. *Cellulose* 20: 2731–2744. DOI: 10.1007/s10570-013-0072-7
- Tahiri C, Vignon MR (2000) TEMPO-oxidation of cellulose: Synthesis and characterization of polyglucuronans. *Cellulose* 7: 177-188. DOI: 10.1023/A:1009276009711

Tomar R, Sharma J, Nishimura S, Ebitani K (2016) Aqueous Oxidation of Sugars into Sugar Acids Using Hydrotalcite-supported Gold Nanoparticle Catalyst under Atmospheric Molecular Oxygen. *Chem Lett* 45: 843-845. DOI: 10.1246/cl.160364

Willker W, Leibfritz D, Kerssebaum R, Bermel W (1993) Gradient Selection in Inverse Heteronuclear Correlation Spectroscopy. *Magn. Reson. Chem.* 31: 287–292. DOI: 10.1002/mrc.1260310315

Wu DH, Chen AD, Johnson CS (1995) An Improved Diffusion-Ordered Spectroscopy Experiment Incorporating Bipolar-Gradient Pulses. *J. Magn. Reson. A* 115: 260–264. DOI: 10.1006/JMRA.1995.1176